Inorganic Chemistry, 2020, 59, 10, 7103–7116. https://doi.org/10.1021/acs.inorgchem.0c00579

Tris(2-pyridyl) Bismuthines: Coordination Chemistry, Reactivity and Anion-Triggered Pyridyl Coupling

Álvaro García-Romero,[†] Alex J. Plajer,[‡] Daniel Miguel,[†] Dominic S. Wright,[‡] Andrew D. Bond,[‡] Celedonio M. Álvarez,[,†] and Raúl García-Rodríguez*[,†]*

[†]GIR MIOMeT-IU, Cinquima, Química Inorgánica, Facultad de Ciencias, Universidad de Valladolid, Campus Miguel Delibes, 47011, Valladolid, Spain.

[‡]Department of Chemistry, University of Cambridge, Lensfield Road, Cambridge, CB2 1EW, U.K.

KEYWORDS tris-pyridyl ligands, bismuthine, hypervalent, main-group ligands, Lewis acidity

ABSTRACT A series of new *tris*(2-pyridyl) bismuthine ligands of the type [Bi(2-py')$_3$] have been prepared, containing a range of substituents at various positions within their pyridyl rings (py′). They can act as *intact* ligands or, as a result of the low C-Bi bond energy, exhibit non-innocent reactivity in the presence of metal ions. Structural studies of Li^+ and Ag^+ complexes show that the coordination to metal ions using their pyridyl-N atoms and to anions using the Lewis acidity of their Bi(III) centers can be modified by the presence of substituents within the 2-pyridyl rings, especially at the 6- or 3-positions, which can block the donor-N or Lewis acid Bi sites. Electron

withdrawing groups (like CF_3 or Br) can also severely reduce their ability to act as ligands to metal ions by reducing the electron donating ability of the pyridyl-N atoms. Non-innocent character is found in the reactions with Cu^+ and Cu^{2+}, resulting in the coupling of pyridyl groups to form bipyridines, with the rate of this reaction being dependent on the anion present in the metal salts. This leads to the formation of Bi(III)/Cu(I) complexes containing hypervalent $[X_2Bi(2\text{-R-py})]^-$ (X = Cl, Br) anions. Alternatively, the *tris*(2-pyridyl) bismuthine ligands can act as 2-pyridyl transfer reagents, transferring 2-py groups to Au(I) and Fe(II).

INTRODUCTION

Tripodal and facially coordinating ligands have found countless applications in modern coordination, organometallic and bioinorganic chemistry.[1] The ubiquitous *tris*-pyrazolyl borates constitute perhaps the best-known class of this type of ligands (Figure 1a).[2] These popular ligands are extremely versatile, as their steric and electronic characteristics can be easily modified through the introduction of substituents in their pyrazolyl moieties. Although less well-studied, *tris*(2-pyridyl)-based ligands have emerged as another important class of tripodal ligands. Most studies in this area in the last 40 years have focused on ligands of the type $E(2\text{-py})_3$ that contain lighter, non-metallic bridgehead atoms (E = CR, COR, CH, N, P, P=O, *etc.*; 2-py = 2-pyridyl; Figure 1b).[3] These ligands have found a broad range of applications in similar areas to their *tris*-pyrazolyl borate counterparts in coordination, catalysis, and organometallic and bioinorganic chemistry, including stoichiometric organic transformations and as models for the coordination in enzymatic metal sites.[4]

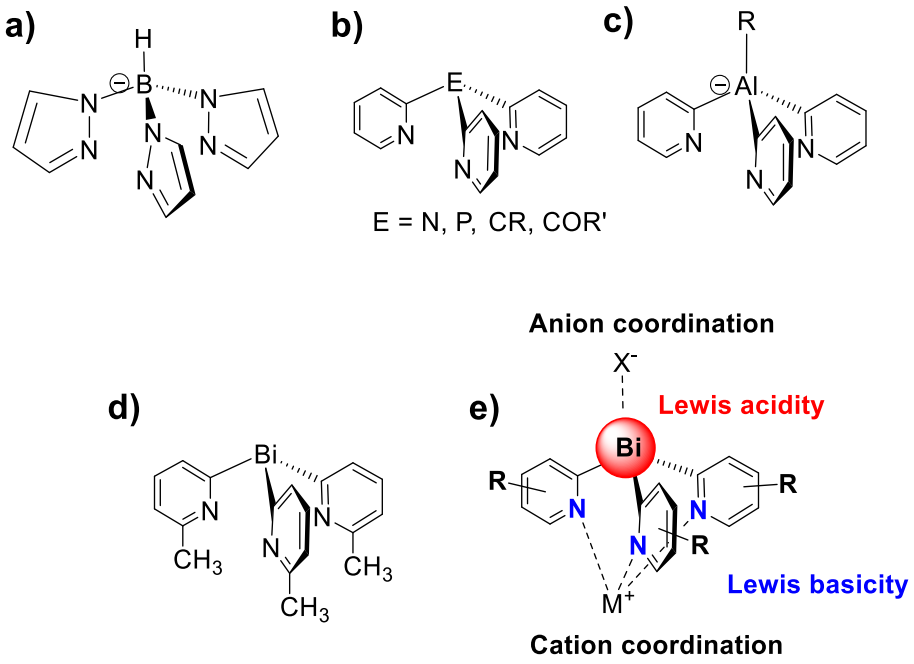

Figure 1. a) The *tris*-pyrazolyl borate ligand, b) "classical" *tris*(2-pyridyl) ligands with non-metallic bridgeheads, c) *tris*(2-pyridyl) aluminates, and d) Bi[(6-Me-2-py)$_3$], the only example of a bismuthine *tris*(2-pyridyl) ligand. e) Introduction of a functional group in the bismuthine framework to modulate Lewis acidity and basicity, which in turn affects the cation and anion coordination ability of the ligand.

More recently, attention has turned to *tris*(2-pyridyl) arrangements containing heavier and more metallic bridgehead atoms.[8–20] The introduction of different main group elements as the bridgehead is a simple and emerging strategy for modifying the reactivity and coordination properties of different types of ligands.[21–23] The introduction of larger (more electropositive) *p*-block bridgeheads can be used to modify the electronic (donor) character and the ligand bite of *tris*(2-pyridyl) ligands in a systematic way.[24] This approach has recently been shown to be of value in modulating the catalytic activity of transition metal complexes of Group 15 *tris*(2-pyridyl) ligands.[25]

One further potential consequence of incorporating more electropositive (metallic and semi-metallic) bridgehead atoms is an increase in the polarity of the bridgehead atom–C bonds to the pyridyl groups. In contrast to more robust *tris*(2-pyridyl) borate ligands,[26–28] *tris*(2-pyridyl)aluminates $[RAl(2\text{-py})_3]^-$ (Figure 1c) react as bases with H_2O, alcohols or carboxylic acids in a controlled manner, providing an interesting route to new aluminates containing additional donor functionality.[29–31] This behavior has led to new applications as thermally stable pyridyl-transfer reagents as well as reagents for the rapid NMR spectroscopic determination of the enantiomeric excess (*ee*) of chiral alcohols.[32–34]

Although the coordination chemistry of *tris*(2-pyridyl) ligands $E(2\text{-py})_3$ of the lighter Group 15 elements (E = N, P, As) has been extensively studied,[35–49] it was only very recently that heavier counterparts containing Sb and Bi have been introduced. Most relevant to the current study, we showed that 6-methyl substitution at the pyridine rings allows the synthesis of the stable ligand $[Bi(6\text{-Me-2-py})_3]$ (**1**) (Fig 1d), which is to date the only example of a *tris*(2-pyridyl) bismuthine reported. Our studies on the coordination chemistry of this new ligand were, however, limited to Cu(I) complexes, and very little is known about the coordination characteristics or reactivity of these species.[25]

Due to the low toxicity[50–52] and the highly Lewis acidic character of bismuth , the chemistry of organobismuth compounds is experiencing a resurgence of interest, finding different applications in catalysis, activation reactions and materials chemistry.[53–61] Nonetheless, bismuthine ligand chemistry remains relatively underdeveloped in comparison to that of lighter Group 15 based ligands, in part due to the weakness of element–Bi bonds, which can make them thermally unstable. Illustrating the potential in this area, Gabbai and Limberg have recently developed amphiphilic bismuthine ligands of the type PBiP (P = phenylenephosphino groups), which utilize

the Lewis acidity of Bi(III) to support unusual donor-acceptor transition metal→Bi bonding.[62–65] Our previous study of the *tris*(2-pyridyl) ligand [Bi(6-Me-2-py)$_3$] (**1**) also shows that it can exhibit amphiphilic character (being capable of coordinating anions and cations simultaneously), as revealed in particular by the unusual structure of the Cu(I) dimer [Bi(6-Me-2-py)$_3$(CuCl)]$_2$ in which the separate monomer units associate by Bi•••Cl interactions.[25]

With this background in mind, we present here a study that allows access to a range of *tris*(2-pyridyl) bismuthines containing different functionalities in the pyridyl rings. We explore how the introduction of different substituents on the pyridyl rings (Figure 1e) can be used to control the steric and electronic properties of the bismuthine ligands, and thus, their reactivity and coordination behavior towards cations and anions.

RESULTS AND DISCUSSION

Our recent success in the synthesis of [Bi(6-Me-2-py)$_3$] (**1**) [25] motivated us in the initial part of this study to test whether a similar synthetic approach could be used to access a range of related bismuthine ligands. This would be the first step towards fine-tuning their electronic and steric properties by the introduction of substituents in the pyridyl rings. We previously attributed the stability of **1** compared to that of the unsubstituted bismuthine ligand (which we were unable to obtain) to the presence of 6-Me groups in the pyridyl rings, as their electron-donating nature prevented reductive elimination of 2,2′-bipyridine and the formation of Bi metal. In the current study we first explored the synthesis of other *tris*(2-pyridyl) ligands containing electron-withdrawing substituents at the 6-position of the pyridyl ring in order to assess their stability in comparison to **1**. In addition to modifying the donor strength and steric profile of the pyridyl coordination site of the bismuthine ligand, we reasoned that the introduction of electron-withdrawing groups should also result in increased Lewis acidity at the bismuth center. The

preparation of the new ligands [Bi(6-R-2-py)$_3$] [R = Br (**2**), CF_3 (**3**), Ph (**4**)] was straightforward from the reaction of $BiCl_3$ and the corresponding 2-lithio-6-substituted-pyridine (2-Li-6-R-py) in THF or Et_2O at -78 °C (see Scheme 1a). The lithiation time and solvent used in the initial lithiation step were found to be the most critical influences on the yield, with **2**-**4** being isolated in 60-88% crystalline yields after workup from these reactions (see Experimental Section).

We also extended this methodology to other 2-pyridyl ligand arrangements *without* 6-substitution (Scheme 1b). In the absence of steric congestion in the proximity of the donor-N atoms of the 2-pyridyl ring units, these new ligands are all isolated as their lithium halide complexes, **5**•LiCl, **6**•LiX, and **7**•LiX, in which X is either Cl or Br, or a mixture of the two (according to X-ray diffraction). To our surprise, although a small amount of black precipitate (presumably Bi metal) is formed in the case of the unsubstituted bismuthine ligand, careful optimisation of the reaction conditions allowed us to obtain the unsubstituted ligand [Bi(2-py)$_3$] (**5**), which had previously eluded ourselves and others.[25,66] In addition, the first examples of 3- and 5-methyl substituted ligand frameworks, [Bi(5-Me-2-py)$_3$] (**6**) and [Bi(3-Me-2-py)$_3$] (**7**), were also obtained. The isolated crystalline yields of the halide complexes of **5**-**7** after workup were in the range 49-74% (see Experimental Section)

Scheme 1. a) Synthesis of 6-substituted *tris*(2-pyridyl) ligands **2**-**4**. b) Synthesis of 3-, 5- and unsubstituted *tris*(2-pyridyl) ligands **5**-**7** (isolated as their lithium halide complexes).

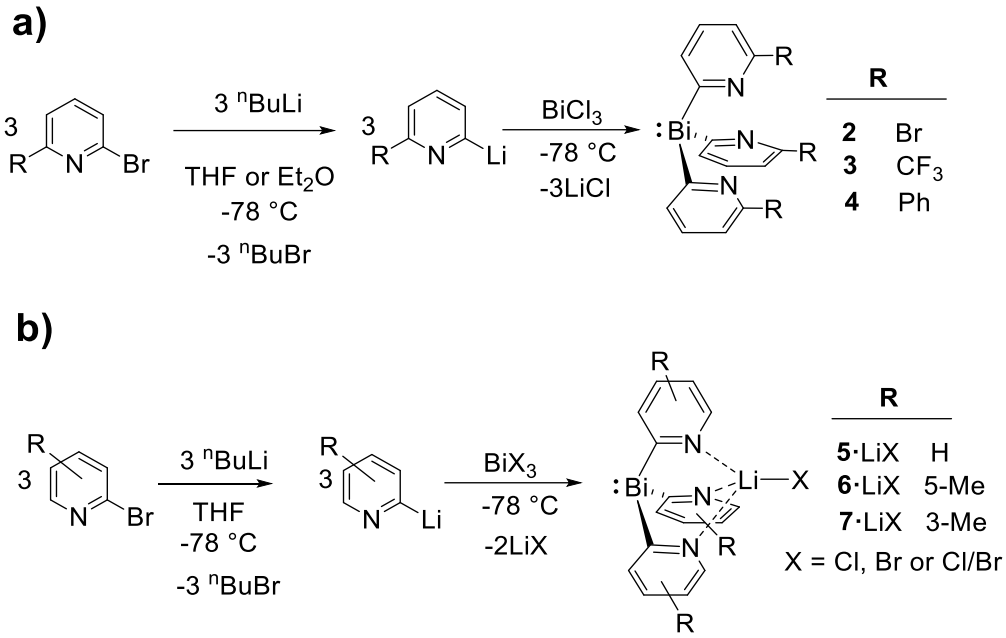

The new compounds **2**-**4** and the lithium halide complexes of **5**-**7** were characterized by a range of NMR spectroscopic and analytical techniques prior to their structural characterization by single-crystal X-ray diffraction (see SI). As expected, the solid-state structures of **2**, **3** and **4** all show pyramidal Bi(III) centers (Figure 2). All the N-pyridyl atoms and 6-substituents are oriented "upwards", approximately towards the bismuth lone pair. The presence of electron-withdrawing groups in **2**-**4** has no significant effect on the bridgehead C-Bi-C angles compared to those of **1** (range 93.2(2)-94.7(4)° in **2**-**4**, cf. 95.0(3)° in **1**). Previous studies have indicated that such acute angles indicate p-character in the C-Bi bonds, and accordingly, s-character in the metal lone pair.[67]

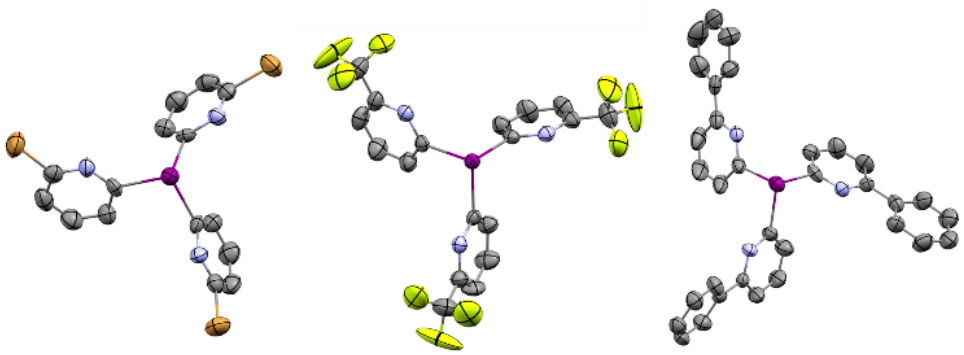

Figure 2. Molecular structures of **2** (left), **3** (center) and **4** (right), showing displacement ellipsoids at 50% probability. H-atoms and the disorder of one of the CF_3 groups in **3** are omitted for clarity. Selected bond lengths (Å) and angles (°): **2**, Bi-C_{py} 2.252(12); C_{py}–Bi–C_{py} 93.7(4). **3**, Bi-C_{py} 2.257(7); C_{py}–Bi–C_{py} 93.2(2). **4**, Bi-C_{py} 2.26(1)-2.23(1); C_{py}–Bi–C_{py} 94.7(4)-92.3(4). Color key: C (grey), Bi (purple), N (blue), Br (brown), F (yellow). See also Table S1 in the SI.

The solid-state structures of the crystalline complexes **5**•LiCl, **6**•LiX•CH_2Cl_2 and **7**•LiX•CH_2Cl_2 are shown in Figure 3. While the single-crystal analysis of **5**•LiCl indicated that Cl^- was the only halide ion present, crystals of **6**•LiX and **7**•LiX were observed with site-disordered mixtures of Cl^- and Br^-. Similar LiX coordination and site disordering of Cl^- and Br^- has been observed during the synthesis of a number of other *tris*(2-pyridyl) ligands and results from the *in situ* generation of LiBr by Cl/Br exchange from the by-product ^{n}BuBr.[9,24] Molecules of each of these complexes consist of LiX units (X = Cl/Br) in which the Li^+ cation is *tris*-coordinated by the three N-atoms of the pyridyl rings of the *tris*(2-pyridyl) bismuthine ligands. The presence of Li^+ in bulk samples of the complexes was confirmed by solution ^{7}Li NMR spectroscopy. Bulk samples of pure LiCl coordination complexes can be obtained by the reactions of the mixed halide complexes with tetrabutyl ammonium chloride. Mixed halide composition can also be avoided by employing $BiBr_3$ as the bismuth source instead of $BiCl_3$. This allowed us to prepare **6**•LiBr and **7**•LiBr without Cl^- inclusion (see Experimental Section and SI).

In **5**•LiCl (Figure 3a) and **6**•LiX (Figure 3b), in which the Bi(III) centers of the *tris*(2-pyridyl) ligands are exposed, short intermolecular Bi•••X contacts[67,68] clearly link the molecules together into a 1-D polymeric arrangement. The coordination geometry around Bi becomes effectively disphenoidal (seesaw), with the intermolecular contact occupying an axial position. Comparable interactions are seen in **7**•LiX (Bi•••Br = 3.833(2) Å), but they are considerably longer on account

of the steric hindrance caused by the 3-Me groups flanking the Bi(III) center (Figure 3c). This shows that substitution at the 3-position of the pyridyl ring can be used to modulate anion coordination to Bi(III) in a similar manner to the way in which 6-substitution can be employed to control cation coordination of the *tris*(2-pyridyl) bismuthine N-atoms (see later).

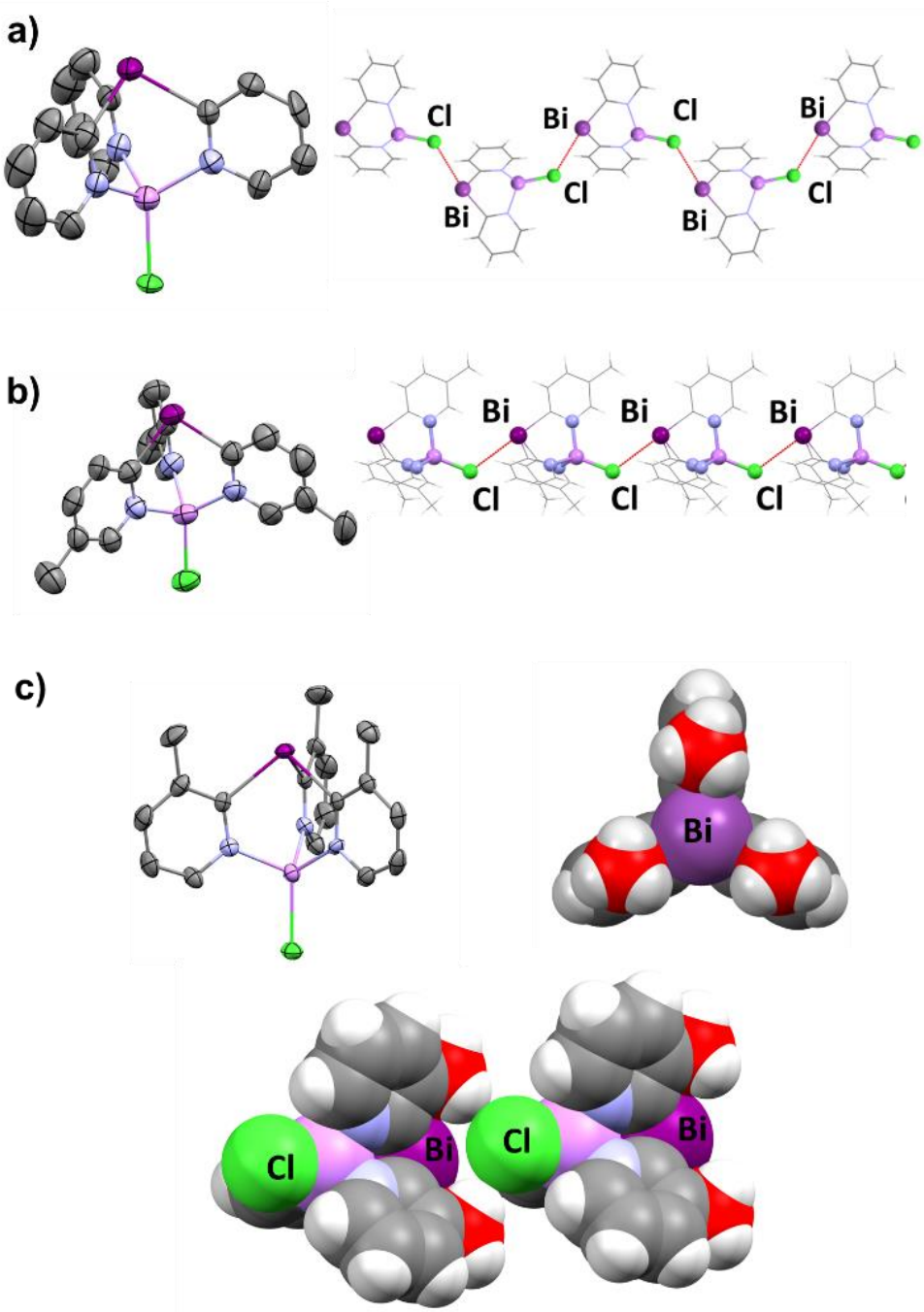

Figure 3. (a, left) Molecular structure of the monomeric unit of **5**•LiCl; displacement ellipsoids at 50% probability. (a, right). View along the b axis and formation of a zig-zag type structure through Bi•••Cl interactions between the monomeric units. (b, left). Molecular structure of **6**•LiX; displacement ellipsoids at 50% probability. Cl/Br disorder is present, with a partial occupancy of 0.6 for Cl and 0.4 for Br. H atoms and the Br component of the disorder, as well as one molecule of CH_2Cl_2 present in the asymmetric unit, are omitted for clarity. See SI for the structure of the pure **6**•LiBr coordination complex. (b, right) View of **6**•LiX along the a axis and formation of a zig-zag type structure through Bi•••Cl interactions of the monomeric units. The Br component of the disorder is omitted for clarity. Both the Bi•••Cl contacts in **5**•LiCl (3.455(2) Å) and the Bi•••Br contacts in **6**•LiBr (3.525(8) Å) are well below the sum of the relevant van der Waals radii (Σ_{VDW}(Bi–Cl) = 3.82, Σ_{VDW}(Bi–Br) = 3.90 Å).[69,70] (c, left) Molecular structure of the monomeric unit of **7**•LiX; displacement ellipsoids at 50% probability. Cl/Br disorder is present, with a partial occupancy of 0.7 for Cl and 0.3 for Br. See SI for the pure LiCl and LiBr coordination complexes. H atoms and the Br component of the disorder, as well as one molecule of CH_2Cl_2 present in the asymmetric unit, are omitted for clarity. See SI for the structures of **7**•LiCl and **7**•LiBr. (c, right) Space-filling view of **7** down the Bi···Li axis with the Li-X unit omitted and the 3-methyl groups highlighted in red. (c, bottom) Space-filling representation of two adjacent **7**•LiX molecules. The Br component of the disorder is omitted for clarity, and the 3-methyl groups are highlighted in red. Selected bond lengths (Å) and angles (°) for **5**•LiCl: Bi-C_{py} 2.266(8)-2.289(10), N--N 3.13(1)-3.154(9); C_{py}–Bi–C_{py} 92.3(4)-93.4(3), Cl---Bi–C_{11py} 170.4(2) for **6**•$LiCl_{0.6}Br_{0.4}$: Bi-C_{py} 2.287(8)-2.257(8), N--N 3.174(8)-3.110(8); C_{py}–Bi–C_{py} 92.6(3)-93.2(3), for **7**•$LiCl_{0.7}Br_{0.3}$: Bi-C_{py} 2.281(6)-2.296(8), N--N 3.115(9)-3.077(9). Color key: C (grey), Bi (purple), N (blue), Li (pink), Cl (green). See also Table S1 in the SI.

Ligands **2**-**4** and the complexes **5**•LiCl, **6**•LiX and **7**•LiX are all thermally stable and can be stored indefinitely in solid form under a N_2 atmosphere. They are also remarkably stable towards moisture. With the exception of **7**, which slowly decomposes in the presence of excess H_2O to generate free 3-Me-2-py-H, the remaining compounds are stable towards moisture, and no hydrolysis was observed two days after the addition of ca. 15 equivalents of H_2O in toluene-d_8 or $CDCl_3$, as monitored by ^{1}H NMR spectroscopy. In fact, decoordination of LiX from ligands **5** and **6** can be accomplished by extraction with toluene/H_2O (Experimental Section). Nominally halide-free ligands **5** and **6** were obtained in this manner, and in the case of **6**, its structure was confirmed by X-ray crystallography (see SI).

The isolation of ligands **5**, **6** and **7** as lithium halide complexes reflects their higher affinity for Li^+, in contrast to the 6-pyridyl substituted ligands **1**-**4,** in which the donor-N atoms of the pyridyl groups are more sterically congested. Upon the addition of increasing amounts of LiCl to $CDCl_3$ solutions of free ligands **5** and **6**, a shift in the pyridyl signals is observed in their ^{1}H NMR spectra indicative of LiCl coordination. This shift is largest for H-6 (*i.e.*, next to the pyridyl nitrogen), which is deshielded by around 0.5 ppm (see Figure 4). These changes are accompanied by the appearance of a singlet at 6.2 ppm in their ^{7}Li NMR spectra resulting from coordination of LiCl to the ligand. In contrast, addition of LiCl to solutions of **1-4** under the same conditions did not result in coordination to LiCl, as evidenced by ^{1}H and ^{7}Li NMR spectroscopy. This indicates that 6-substitution of the pyridyl ring completely blocks the coordination of LiCl. This may be due in part to the poorer donor ability of the pyridyl N atoms in the bismuthine ligands **2** and **3** (as a result of the presence of electron-withdrawing Br and CF_3 groups), but it is also likely to be steric in origin.

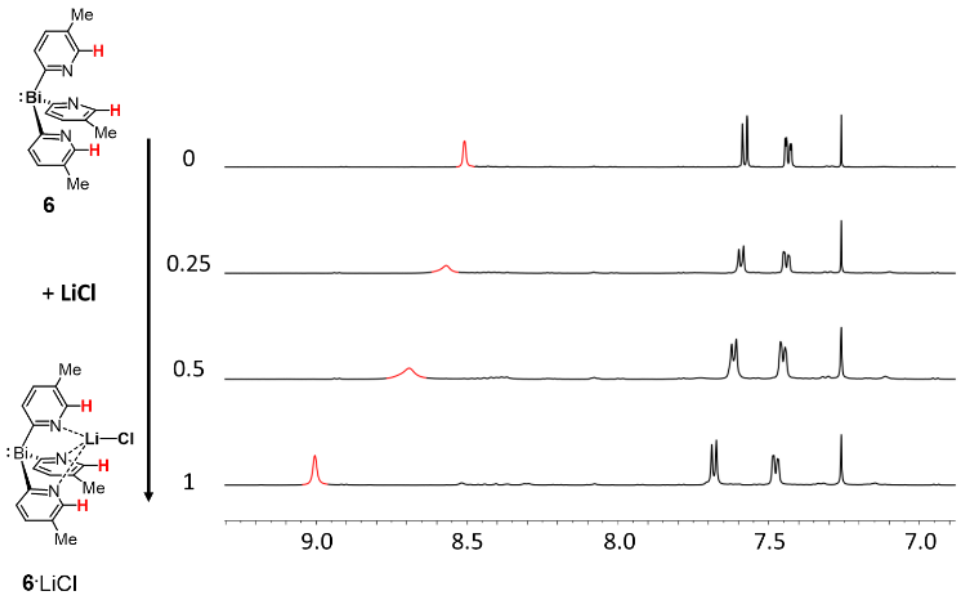

Figure 4. ^{1}H NMR spectra of the successive addition of LiCl to a solution of free ligand **6**. LiCl coordination is evident from the observed shifts of the signals. H-6 (i.e., next to the pyridyl nitrogen, highlighted in red) exhibits the largest shift of around 0.5 ppm. The spectrum for 1 eq. LiCl is identical to that of **6**•LiCl in $CDCl_3$. No further changes to the spectrum were observed when >1 eq. LiCl was added.

With the new ligands **1** and **2**-**7** in hand, we next explored their coordination to a range of metals. Reactions of **1** with equimolar amounts of AgOTf, $AgBF_4$ or $AgPF_6$ in MeCN give the new complexes [Bi(6-Me-2-py)$_3$Ag(MeCN)]OTf (**8**•OTf), [Bi(6-Me-2-py)$_3$Ag(MeCN)]BF_4 (**8**•BF_4) and [Bi(6-Me-2-py)$_3$Ag(MeCN)]PF_6 (**8**•PF_6) (Scheme 2). Similar reaction of **4** with $AgBF_4$ in MeCN gives [Bi(6-Ph-2-py)$_3$Ag(MeCN)]BF_4 (**9**•BF_4). In contrast to ligands **1** and **4**, no coordination was observed between bismuthine ligands **2** or **3** and AgX salts (X = OTf, BF_4, PF_6). Bearing in mind that the van der Waals radius of CH_3 (2.23 Å) is intermediate between those of CF_3 (2.74 Å) and Br (1.85 Å),[69,71] the inability of ligands **2** and **3** to coordinate Ag^+ most likely arises from the electron-withdrawing nature of the substituents (*i.e.*, reducing the donor ability) rather than just steric hindrance of the coordination site. This point is emphasized by the fact that

despite its sterically hindering groups, **4** readily forms the Ag(I) complex [Bi(6-Ph-2-py)$_3$Ag(MeCN)][BF$_4$] (**9**•BF$_4$) with AgBF$_4$. The lithium halide complexes **5**•LiX, **6**•LiX and **7**•LiX proved to be very poor sources of the ligands **5**, **6** and **7** since the halide ions interfered significantly in the transmetallation reactions with Ag^+ salts. For example, reactions with AgOTf in acetonitrile resulted in halogen/OTf anion exchange with the precipitation of AgCl and formation of LiOTf complexes, as shown by multinuclear NMR studies and the solid-state characterization of the LiOTf complex of **6** (see SI). The reaction between lithium-halide-free ligand **5** and Ag(OTf) in acetonitrile resulted in the precipitation of a white solid, suggesting the formation of a silver complex. However, this was highly insoluble and could not be characterized.

The room-temperature ^{1}H NMR spectra of the Ag^+ complexes **8** and **9** in acetonitrile-d$_3$ both show the presence of only one pyridyl environment. The pyridyl resonances are shifted downfield with respect to those of the free ligands **1** and **4**, indicating coordination to Ag. In the case of complex **8**, the presence of different anions (OTf^-, BF_4^- and PF_6^-) does not substantially affect the ^{1}H chemical shifts of the pyridyl resonances.

Scheme 2. Synthesis of the silver complexes **8**•X and **9**•BF$_4$.

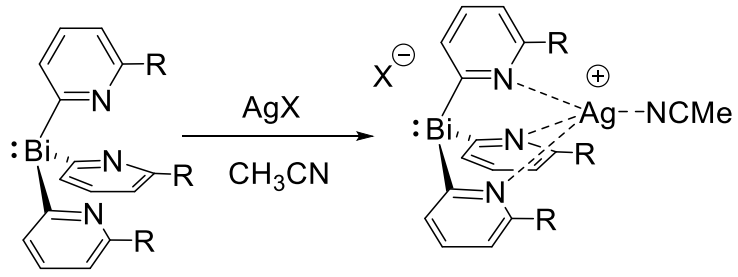

	R	X$^-$
8·OTf	CH_3	**OTf**
8·BF$_4$	CH_3	**BF$_4$**
8·PF$_6$	CH_3	**PF$_6$**
9·BF$_4$	Ph	**BF$_4$**

R = CH_3 (**1**)
R = Ph (**4**)

The solid-state structures of the crystalline complexes **8**•OTf•MeCN, **8**•BF$_4$, **8**•PF$_6$•2CH$_3$CN and **9**•BF$_4$ have ion-separated arrangements consisting of [{Bi(6-Me-2-py)}AgCH$_3$CN]$^+$ or [{Bi(6-Ph-

2-py)$_3$}AgCH$_3$CN]$^+$ cations and the corresponding anions. Their complex cations contain Ag$^+$ centers that are coordinated by the three pyridyl-N atoms of the ligands and by a molecule of MeCN (Figure 5). The structural arrangement of these silver complexes is related to that found previously for the ion-separated Cu(I) complexes [{E(6-Me-2-py)$_3$}Cu•CH$_3$CN]$^+$PF$_6^-$ (E = As, Sb, Bi).[25] However, it differs from that of the silver complex [Ag@Ag$_4$(2-py$_3$P)$_4$(OTf)$_4$](OTf) cluster, in which the *tris*(2-pyridyl) phosphine ligand [P(2-Py)$_3$] coordinates Ag(I) through the pyridines and the phosphorus lone pair.[72] In the bismuthine silver complexes **8**•X (X = OTf$^-$, BF$_4^-$ and PF$_6^-$) and **9**•BF$_4^-$ the low energy of the 6*s* orbitals of the lone pairs of the bismuthine ligands results in no coordination to the soft Ag(I) centers. Instead, the greater Lewis acidity at the bismuth bridgehead atoms can result in solvent•••Bi and anion•••Bi interactions (as also observed in the LiX complexes of **5**-**7**).

Varying degrees of cation-anion interactions are found in **8**•OTf, **8**•BF$_4$ and **8**•PF$_6$. In **8**•OTf (Figure 5a), the Bi(III) bridgehead is involved in an additional long-range interaction with one O-atom of a OTf$^-$ anion and with the N-atom of an MeCN ligand. The Bi-N (3.309(6) Å) and Bi-O (3.326(6) Å) distances involved are longer than expected for donor-acceptor or coordination bonds but significantly shorter than the sum of their van der Waals radii (3.62 and 3.59 Å, respectively). Moving to the less coordinating anions BF$_4^-$ and PF$_6^-$, the Bi(III)•••anion interactions are no longer present (see SI). In **8**•PF$_6$•2CH$_3$CN the Bi(III) bridgehead is coordinated by two MeCN ligands only and in **8**•BF$_4$ no secondary interaction is found with BF$_4^-$ (see SI).

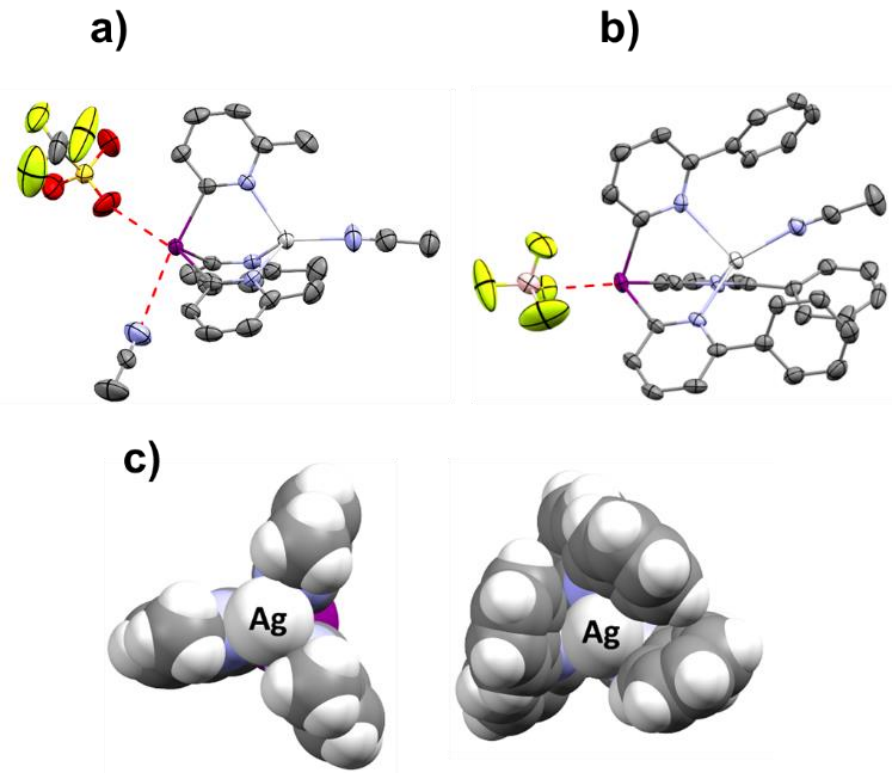

Figure 5. (a) Molecular structure of complex **8**•OTf ([Bi(6-Me-2-py)$_3$Ag(MeCN)]OTf); displacement ellipsoids at 50% probability. (b) Molecular structure of complex **9**•BF_4 [Bi(6-Ph-2-py)$_3$Ag(MeCN)] [BF_4]; displacement ellipsoids at 50% probability. H atoms are omitted for clarity. (c) Space-filling views of the cations [Bi(6-Me-2-py)$_3$Ag(MeCN)] [**8**]$^+$ (left) and [Bi(6-Ph-2-py)$_3$Ag(MeCN)] [**9**]$^+$ (right) down the Ag•••Bi vector. Selected bond lengths (Å) and angles (°) for **8**•OTf: Bi-C_{py} 2.274(5)-2.288(5), N--Ag 2.307(5)-2.380(4); C_{py}–Bi–C_{py} 93.3(2)-99.0(2), O---Bi–C_{11py} 168.7(2), $N_{acetonitrile}$---Bi–C_{21py} 168.6(2) for **9**•BF_4: Bi-C_{py} 2.258(5)-2.273(4), N--Ag 2.337(3)-2.464(3); C_{py}–Bi–C_{py} 94.9(2)-96.7(2), F---Bi–C_{21py} 175.7(1). Color key: C (grey), Bi (purple), N (blue), Ag (light grey), F (yellow), B (pink), O (red).

The use of the more sterically congested bismuthine ligand **4** results in the significantly distorted cation **9**•BF_4 (Figure 5b). An indication of this is seen in the coordination of the molecule of MeCN to the Ag center, which is tilted away from the Bi•••Ag•••N axis (Bi-Ag-N angle 162.4(1)°), unlike

in the cations [**8**]$^+$ in which the Bi•••Ag•••N fragment is almost linear (Bi•••Ag•••N range 176.1(2)-175.3(2)°). No expansion of the C_{py}-Bi-C_{py} angles is observed in the cation [**9**]$^+$ (94.9(2)-96.7(2), cf. 93.3(2)-100.4(2) for cations [**8**]$^+$), and therefore the coordination of the MeCN molecule to Ag^+ must be accomplished by distortion of the pyridyl coordination environment. A large twist of 49.2° in one of the Py units with respect to the Bi•••Ag axis occurs, which in turn results in the elongation of the coordinating N-Ag bonds (2.464(3) Å, cf. N-Ag distances in the range 2.307(5)-2.380(4) Å for the cations [**8**]$^+$). Figure 5c shows the cations [**8**]$^+$ and [**9**]$^+$ along their Ag-acetonitrile axes and illustrates the more sterically constrained nature of the coordination environment around the Ag(I) center in cation [**9**]$^+$ as compared to cations [**8**]$^+$. Recently, there has been great interest in closed-shell metal-Bi interactions.[48,65,73–75] In this regard, seemingly short Bi•••Ag contacts are present in the cations [**8**]$^+$ and [**9**]$^+$ (range 3.6746(6)-3.7291(4), cf. 3.79 Å for Σ_{VDW}). However, it is likely that these interactions are weak at best in this case.

Further investigations of the coordination behavior of these bismuthine ligands towards the other coinage metals, copper and gold, illustrate the non-innocent nature of some of these ligands, which are subject to either 2-pyridyl ligand transfer or reductive elimination. While the silver complexes **8**•X (X = OTf^-, BF_4^-, PF_6^-) and **9**•BF_4 are stable in rigorously dried CH_3CN in an N_2 atmosphere, the corresponding Cu(I) complexes of ligands **1** and **4** were found to be less stable. Prolonged storage of the 1:1 reaction between $[Cu(MeCN)_4]BF_4$ and bismuthine ligand **1** at room temperature in MeCN led to a gradual color change from pale yellow to orange, with the formation of a few red and yellow crystals and a black precipitate. X-ray analysis shows that the red crystals are the copper(I) complex $[Cu(Me\text{-}bpy)_2]BF_4$ (Me-bpy = 6,6'-dimethyl-2,2'-bipyridyl),[76] while the yellow crystals are the unusual Bi(III)/Cu(I) complex $[\{Bi(6\text{-}Me\text{-}2\text{-}py)_3Cu\}Cu(Me\text{-}bpy)](BF_4)_2$ (**10**•$(BF_4)_2$). The $[\{Bi(6\text{-}Me\text{-}2\text{-}py)_3Cu\}Cu(Me\text{-}bpy)]^{2+}$ dication [**10**]$^{2+}$ (Figure 6) consists of a

[Bi(6-Me-2-py)$_3$Cu] subunit in which the Cu(I) center is only coordinated by two of the three 2-pyridyl N-atoms, with the third pyridyl-N atom coordinating the Cu(I) center of a [Cu(Me-bpy)]$^+$ unit, giving rise to two trigonal planar Cu(I) environments. No π-arene-Cu(I) interactions are present in this arrangement.

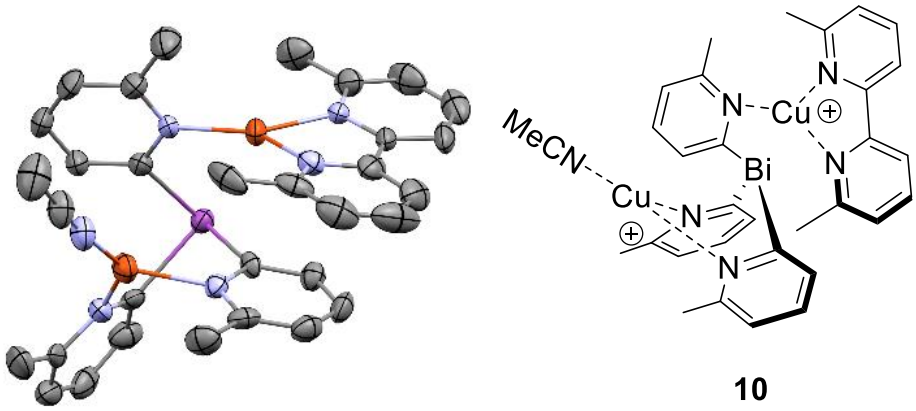

10

Figure 6. (left) Solid-state structure and (right) line drawing of complex dication [**10**]$^{2+}$. Displacement ellipsoids shown at 50% probability; H atoms and two BF_4^- anions omitted for clarity. Selected bond lengths (Å) and angles (°): Bi-C_{py} 2.259(6)-2.291(9), C_{py}–Bi–C_{py} 90.4(3)-91.7(3). Color key: C (grey), Bi (purple), N (blue), Cu (orange).

The formation of a bipyridine molecule as a ligand in the cation of **10** must result from reductive elimination, presumably from the initially formed [Bi(6-Me-2-py)$_3$Cu(MeCN)]$^+$ cation in the manner illustrated in Scheme 3. This was proved by *in situ* ^{1}H NMR spectroscopic investigation of the 1:1 reactions of **1** and **4** with [Cu^{I}NCMe]BF$_4$ or Cu^{I}Cl in acetonitrile-d$_3$ under N$_2$ at room temperature. Upon mixing [Cu(MeCN)$_4$]BF$_4$ and the bismuthine ligands **1** or **4**, immediate formation of the complexes [Bi(6-Me-2-py)$_3$CuNCMe]BF$_4$ and [Bi(6-Ph-2-py)$_3$CuNCMe]BF$_4$ was observed (see SI). After 7 and 5 days, respectively, very small amounts of the corresponding bipyridines Me-bpy and 6,6′-diphenyl-2,2′-dipyridyl (Ph-bpy) were formed. Much faster reaction occurs using CuCl instead of [Cu(MeCN)$_4$]BF$_4$. The reaction of **4** and CuCl (1:1) in MeCN

immediately turned red and the ^{1}H NMR spectrum showed the formation of Ph-bpy within the first 10 min. After 24 h at room temperature, the ^{1}H NMR spectrum shows the almost exclusive formation of Ph-bpy, together with unidentified minor products and with the appearance of a black precipitate (see later discussion). Similar observations were made in the reaction between **1** and CuCl. In this case, however, the formation of Me-bpy proceeded more slowly, and after 5 days at room temperature *ca* 80% conversion had occurred.

Scheme 3. Reductive elimination from the 2-pyridyl ligands of **1** and **4** (X = Cl^{-}, BF_4^{-}).

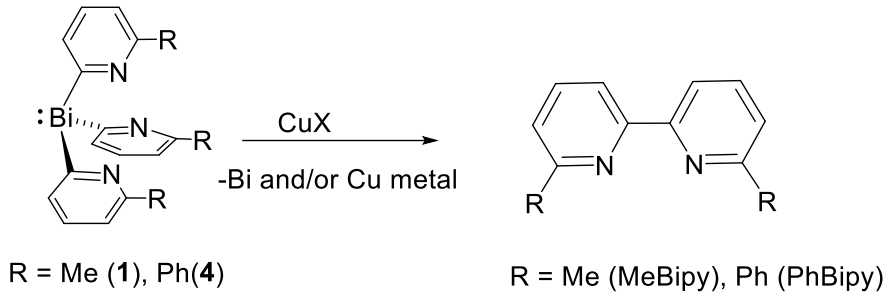

R = Me (**1**), Ph(**4**)

R = Me (MeBipy), Ph (PhBipy)

An intriguing observation in these reactions is the marked effect of the anion on the rate of these coupling reactions. As seen in our previous study of the coordination chemistry of [Bi(6-Me-2-py)$_3$] with CuX (X = Cl^{-}, PF_6^{-})[25] as well as in the current study with Ag(I) and Li salts, the Bi(III) bridgehead atom is sufficiently Lewis acidic to interact with anions. The presence of the more strongly coordinating chloride ligand in CuCl (as compared to weakly coordinating BF_4) could potentially trigger ligand coupling by the transfer of the halogen to the Bi(III) center, forming more reactive hypervalent bismuthate species which facilitate the transfer of the 2-pyridyl groups and reductive elimination to bipyridines.

The black precipitate formed in these reactions could be Bi(0) and/or Cu(0). In this regard, Cu(II)-mediated coupling of pyridyl anions to bipyridines is a well-established synthetic protocol, and one plausible mechanism for the coupling of the pyridyl groups in our study involves the disproportionation of Cu(I) into Cu(0) and Cu(II), with subsequent Cu(II)-mediated coupling.[77,78]

To explore this possibility further, $CuCl_2$ was reacted with ligand **1** (1:1 equivalents) in acetonitrile at room temperature. The solution immediately turned red, and orange crystals of the product [Cu^{I}(MeCN)(μ-Cl)(6-Me-2-Py)$_2$$Bi^{III}$Cl)] (**11a**) were obtained in 40% yield. The reaction of ligand **3** with $CuCl_2$ under the same conditions gave the closely related complex [Cu^{I}(MeCN)(μ-Cl)(6-CF_3-2-Py)$_2$$Bi^{III}$Cl)]•MeCN (**11b**•MeCN), although in this case three equivalents of $CuCl_2$ were required and unreacted ligand **3** was still present in the reaction mixture. The analogous complex [Cu^{I}(MeCN)(μ-Cl)(6-Me-2-Py)$_2$$Bi^{III}$Br)]•$CH_2Cl_2$ (**11c**•CH_2Cl_2) was obtained from the reaction of ligand **2** with $CuBr_2$ in 24% crystalline yield. *In situ* ^{1}H NMR spectroscopy confirmed the formation of the corresponding bipyridine products in each of the reactions producing **11a-11c** (Scheme 4). Compounds **11a-11c** are stable in MeCN solution even in the presence of aerial oxygen for several days, after which slow formation of the free pyridines was observed by ^{1}H NMR spectroscopy. Significantly, no formation of the bipyridines was observed, proving that the coupling reaction does not result from the effect of adventitious oxygen or moisture on **11a-11c** (*i.e.*, they are not intermediates in the coupling reaction). Although organobismuth compounds can mediate different carbon-carbon bond forming reactions, bismuthine ligand **1** is thermally stable and no decomposition or coupling reaction to produce Me-bpy was observed after heating a sample of 1 in acetonitrile at 80 C for 24 h.[79]

Scheme 4. Formation of **11a**, **11b** and **11c**.

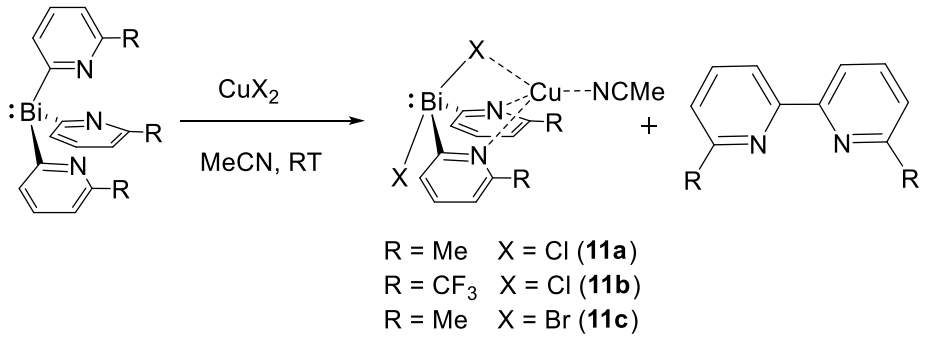

R = Me X = Cl (**11a**)
R = CF_3 X = Cl (**11b**)
R = Me X = Br (**11c**)

Complexes **11a, 11b and 11c** are isostructural, having a Bi(III)/Cu(I) arrangement which consists of an ion-pair between hypervalent $[X_2Bi(2\text{-}R\text{-}py)_2]^-$ (X = Cl, Br) anions and the $Cu(MeCN)^+$ cation, nicely illustrating the ability of the newly- formed pyridine bismuthine ligands to simultaneously coordinate anions and cations. Figure 7a shows the structure of **11a**. As expected, the Bi(III) centers within these anions adopt similar distorted trigonal-bipyramidal geometries with the Bi lone pair formally occupying an equatorial position and the (most electronegative) halogen ligands axial (consistent with VSEPR theory). The Cu(I) centers are coordinated by the two pyridyl-N atoms of the $[X_2Bi(2\text{-}R\text{-}py)_2]^-$ anions and by one of the halogen atoms. Support for the conclusion that these complexes contain hypervalent $[X_2Bi(2\text{-}R\text{-}py)_2]^-$ anions is seen in a comparison in the Bi-X bond lengths within the Cu-(μ-X)-Bi bridges, these bonds being similar to those seen previously in the few known examples of structurally characterized $[X_2BiR_2]^-$ anions, *e.g.*, Bi-Cl 2.688(3) and 2.773(3) Å in **11a**, cf. 2.674(2) Å and 2.800(2) Å in $[Cl_2BiAr_2]^-$ (Ar = 2-methylphenyl).[80] Overall, two important points are illustrated by the formation and structures of **11a**-**11c**: the coupling reaction of the 2-pyridyl groups is likely (at least in part) to involve Cu(II) (via disproportionation of 2Cu(I) → Cu(0) + Cu(II)), and that pyridyl-bismuthine ligands of this type can indeed function as fully-fledged amphiphilic ligands.

In the crystal lattices of the solvates **11b**•CH_3CN and **11c**•CH_2Cl_2 (which crystallize in the non-chiral space groups $P2_1/c$ and P-1, respectively) the monomer units are linked via Bi•••Cl or Bi•••Br interactions. Molecules of **11b** associate into zig-zagged polymers via Bi•••Cl interactions (3.458 Å, cf. Σ_{VDW} = 3.82 Å) while in **11c** this association only occurs to form very loosely linked dimers in which the Bi•••Br distance is at the very limit of the van der Waals distance [(Bi•••Br 3.872, cf. 3.9 Å for Σ_{VDW}(Br-Bi)] (see SI). The Bi atoms of **11b**•CH_3CN are also involved in long-range Bi•••N interactions with the lattice CH_3CN molecules.

In contrast, **11a**•CH_3CN, which, like **11b** and **11c**, is an achiral complex, crystallizes in the tetragonal chiral space group $P4_1$ (Fig 7a) in which the molecules associate via Bi•••Cl interactions into chiral helical polymers formed by four molecules of **11a** around crystallographic 4_1 screw axes. This leads to the formation of a right-handed helix (anticlockwise looking down the crystallographic c axis). Whereas only the terminal Cl atom is involved in the Bi•••Cl interactions in **11b**, both the terminal and μ-Cl atoms are involved in the intermolecular interactions in **11a** (Bi•••Cl mean 3.589 Å). Further analysis of samples of **11a** allowed us to obtain the crystal structure of the other enantiomorph, which crystallizes in space group $P4_3$ in crystals containing solely the left-handed helix (see SI). Compound **11a** is an example of crystalline enantiomorphism emerging from an achiral complex.[81,82]

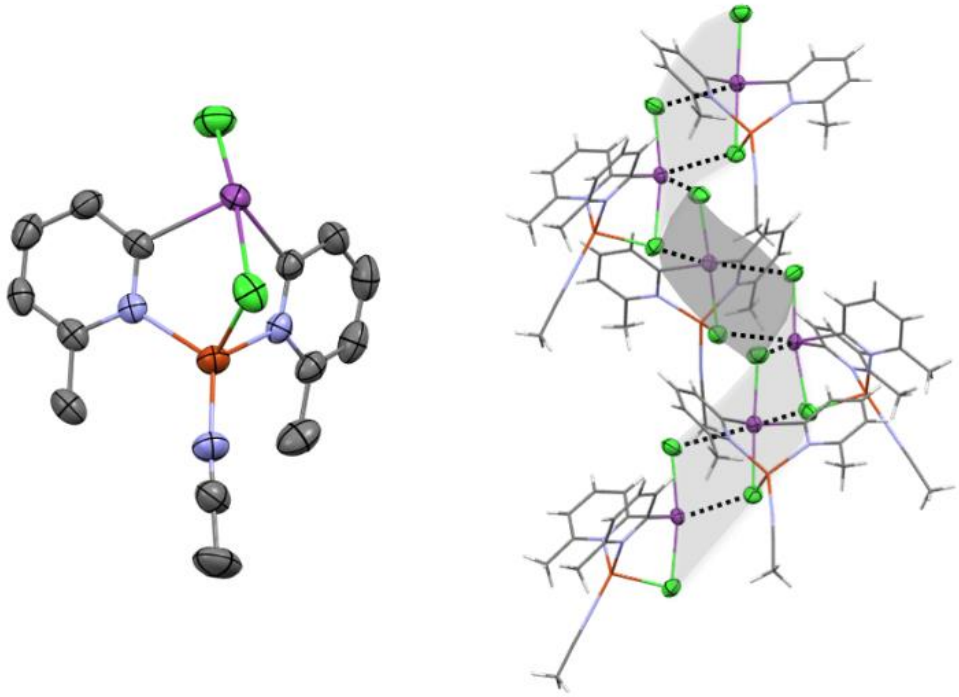

Figure 7. (a) Solid-state structure of complex **11a**. Compounds **11b** and **11c** are isostructural (see SI). Displacement ellipsoids shown at 50% probability; H-atoms and one molecule of MeCN are omitted for clarity. (b) Association of molecules of **11a** in the lattice (the right-handed helix present

in $P4_1$ is shown; for details of the helical arrangement with the opposite handedness, see SI). Selected bond lengths (Å) and angles (°): Bi-C_{py} 2.30(1)-2.28(1), N--Cu 2.03(1)-2.05(1); C_{py}–Bi–C_{py} 92.1(4), Cl–Bi–Cl 169.19(13), Cl---Bi–C_{py} 165.9(3). Color key: C (grey), Bi (purple), N (blue), Cu (orange), Cl (green).

A related structural arrangement to **11a-11c** is formed in the 1 : 1 reaction of **1** with $FeCl_2$ to give the heterometallic Bi(III)/Fe(II) complex [ClBi(6-Me-2-Py)$_2$FeCl$_2$] (**12**) (Figure 8a). This reaction results in significant decomposition and the formation of a black precipitate, presumably of Bi and/or Fe metal or even Bi-Fe intermetallic compounds. The observation of the formation of black precipitates throughout these studies could be due to the formation of Bi-transition metal intermetallics, which could echo recent findings by Vela in the synthesis of 10−14, 10−15 and 11−15 binary intermetallics from heterobimetallic single-source precursors.[83,84] The low isolated yield of **12** meant that it was only characterized by X-ray crystallography. The formation of **12** presumably results from metal-halogen transfer from Fe(II) to Bi(III). However, because of the paramagnetic nature of the reaction solution, we were not able to determine the presence of Me-bpy in solution, and it is therefore unknown whether any pyridyl coupling occurs in this case. In the structure of **12**, the Fe^{II} and Bi^{III} atoms are bridged by 6-Me-2-py groups and by a μ-Cl atom, with both Bi(III) and Fe(II) having trigonal bipyramidal geometries (in the case of Bi(III), the fifth position is formally occupied by the lone pair). Compound **12** forms a 1-D zig-zagged polymer in the crystal lattice via Bi•••Cl interactions between the monomer units (see SI).

Metal-halogen transfer is also observed in the reaction of FeI_2 with **1**, from which a few crystals of Bi[(6-Me-2-py)$_2$HI$_2$] (**13**) were isolated and structurally characterized by X-ray crystallography. Like **12**, **13** contains a hypervalent Bi(III) center (Figure 8b) and can be regarded as an advanced state of the situation seen in the structure of **12**, in which full transfer of the halogen (iodine) from

the Fe(II) to the Bi(III) center has occurred. This leads to the formation of an anionic bismuthate complex $[I_2Bi(6\text{-Me-2-Py})_2]^-$, which is then protonated at one of the pyridyl-N atoms in the reaction medium to give **13** (with the resulting formation of a relatively strong N-H•••N hydrogen bond between the two pyridyl groups). Dimerization of these units occurs in the solid state *via* intermolecular Bi-I•••Bi interactions (3.7988(6) Å, cf. 4.05 Å for the sum of their VdW radii) (Figure 8c).

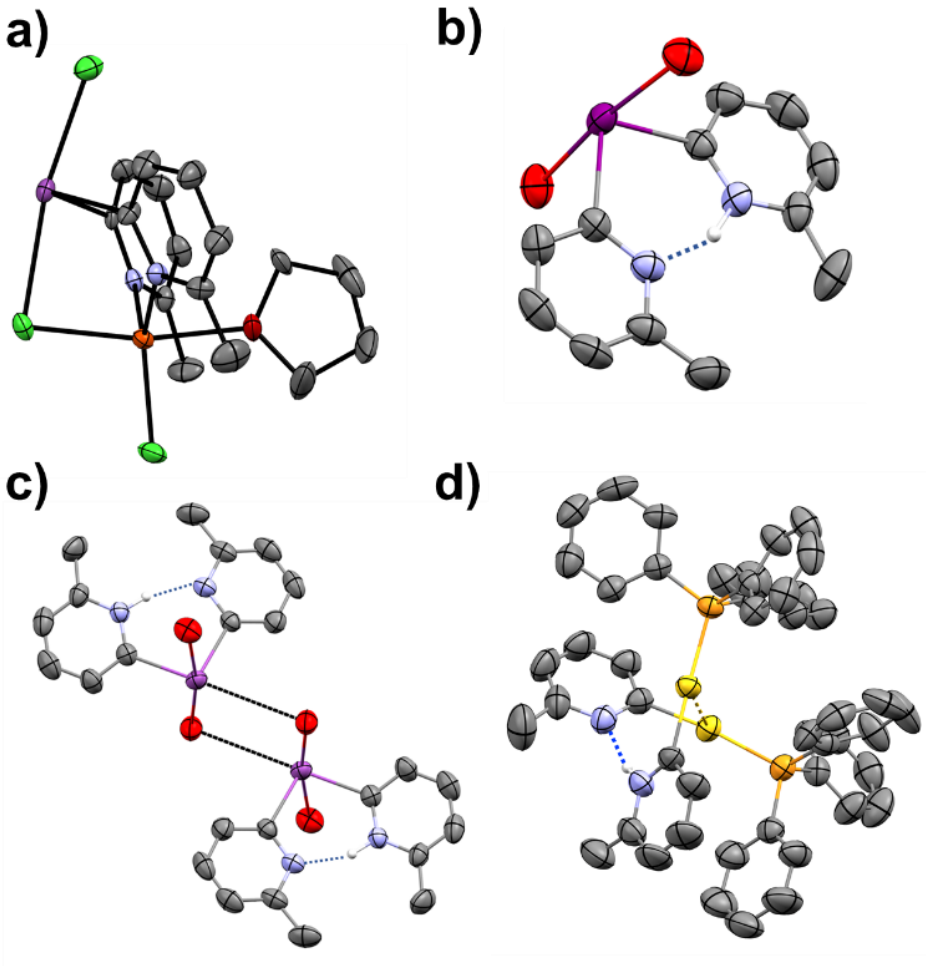

Figure 8. (a) Molecular structure of $[ClBi(6\text{-Me-2-Py})_2FeCl_2]$ (**12**). H-atoms have been omitted for clarity. Thermal ellipsoids at 50% probability. (b) Solid state structure of **13** and (c) its association into dimers through Bi---I intermolecular interactions. Displacement ellipsoids shown at 50% probability. H atoms (except H1) are omitted for clarity. (d) Solid state structure of the

gold pyridyl cation [{(6Me-2-Py)Au(PPh_3)}$_2$H] [**14**]$^+$. H atoms (except H1) and the OTf anion are omitted for clarity. Displacement ellipsoids shown at 50% probability.. Selected bond lengths (Å) and angles (°): **12**, Bi-C_{py} 2.298(8)-2.287(7), N--Fe 2.144(6)-2.151(6); C_{py}–Bi–C_{py} 92.1(2), Cl–Bi–Cl 170.13(6), Cl---Bi–C_{1py} 164.18(6). **13,** Bi-C_{py} 2.286(6), 2.281(7), C_{py}–Bi–C_{py} 94.3(2), I---Bi–C_{11py} 170.5(2). Owing to difficulties with the structure refinement, no bond lengths or angles are quoted for compound **14**•OTf Color key: C (grey), Bi (purple), N (blue), Au (yellow, P (light orange), Fe (dark orange), O (dark red), Cl (green), I (red).

The ability for *tris*(2-pyridyl) ligands to act as pyridyl transfer reagents has been seen previously in the case of the highly reactive and moisture-sensitive [MeAl(2-py)$_3$]$^-$ anion[33,61] and is symptomatic of low bond energy of the C-bridgehead bonds in ligands containing more electropositive (metallic) bridgehead atoms. The ability for **1** to act in a similar way is seen in the example of its reaction with Au(I) salts. While the reaction of **1** and ClAu(tht) (tht = tetrahydrothiophene) in THF led to the formation of an intractable yellow precipitate that could not be further investigated due to its marked insolubility, reaction of (OTf)AuPPh$_3$ with **1** in acetone resulted in a mixture of compounds as shown by ^{1}H NMR, including the appearance of an unexpected broad resonance at δ = *ca.* 12 ppm. After storing the reaction mixture for 48 h at -25 °C, a few crystals of the new compound [{(6Me-2-Py)Au(PPh_3)}$_2$H][OTf] (**14**•OTf) were formed. Despite difficulties in its collection and refinement (due to modelling of disordered triflate; see SI), the single-crystal X-ray data of **14**•OTf define its structure unambiguously. The solid-state structure shows that **14**•OTf has an ion-separated arrangement containing the cation [{(6-Me-2-Py)Au(PPh_3)}$_2$H]$^+$ (**14**) (Figure 8d) and OTf$^-$ anions. The cation consists of a (pyridyl)Au-Au(pyridyl) bonded dimer arrangement in which one of the pyridyl-N atoms is protonated, resulting in an overall positive charge and the formation of a relatively strong N-H•••N hydrogen

bond (similar to **13**). The pyridyl transfer from bismuthine **1** to Au(I) is consistent with previous observations by Schmidbaur, in which the coordination of tertiary bismuthanes (R_3Bi:) to Au(I) was prevented by rapid transmetallation, leading to the formation of organogold compounds.[85]

CONCLUSIONS

The particular interest in *tris*-pyridyl bismuthine ligands of the type [Bi(2-py′)$_3$] is their ability to behave as amphiphilic ligands that are capable of coordinating anions at the Lewis acid Bi(III) bridgehead and at the same time coordinating cations at the donor-N atoms. Our study has provided a range of bismuthine ligands of this type beyond the single example previously reported, illustrating that a range of electron-donating and -withdrawing groups can be introduced into the pyridyl frameworks at various positions. Importantly, we find that 6-Me substitution is not essential for the stabilization of these ligands and that even the unsubstituted ligand **5** is thermally stable. The nature of the substituents (electron-donating or -withdrawing and the steric effects) has a significant impact on the ligand properties. For example, the introduction of 6-Br and 6-CF_3 groups in the ligands **2** and **3** severely curtails the donor ability. Conversely, substitution at the 3-position in the ligand **6** sterically shields the Bi(III) center and reduces its ability to coordinate anions. These features allow control of the coordination ability of the ligand regarding both cation and anion coordination.

The weakness of the C-Bi bonds in these ligands is expressed in their reactions with Cu(I/II), Fe(II) and Au(I). In the case of Cu(I), coupling of the pyridyl groups to the corresponding bipyridines is observed, the rate of which is dependent on the anion present in the Cu(I) salt used. This reaction most probably involves disproportionation of Cu(I) to Cu(II) and Cu(0), as illustrated by the reactions of 6-substituted **1** and **3** with $Cu^{II}X_2$ (X = halide) which results in both pyridyl coupling and the formation of Cu(I) complexes containing hypervalent Bi(III) $[X_2Bi(2\text{-R-py})]^-$

species. A related characteristic is the ability of the bismuthine frameworks to exchange ligands, undergoing metal-halogen or pyridyl transfer with Fe(II) and Au(I) salts.

Overall, this study provides a range of *tris*(2-pyridyl) bismuthines and reveals their interesting coordination and reaction characteristics (as well as their limitations) as ligands. We are continuing our studies in this area, particularly in respect to the use of p-block *tris*(2-pyridyl) species as reagents for chiral discrimination, in supramolecular chemistry and catalysis.

EXPERIMENTAL SECTION

General Experimental Techniques

All syntheses were carried out on a vacuum line under a N_2 atmosphere. Products were isolated and handled under a N_2 atmosphere. Liquid pyridines, NMR solvents, and reaction solvents were stored over molecular sieves and degassed by three freeze-pump-thaw cycles under N_2 prior to use. [Bi(6-Me-2-py)$_3$] (**1**) was synthesized as described previously. NMR spectra were recorded on 500 MHz Agilent DD2 instruments equipped with a cold probe and a 400 MHz Agilent instrument equipped with a ONEPROBE in the Laboratory of Instrumental Techniques (LTI) Research Facilities, University of Valladolid. Chemical shifts (δ) are reported in parts per million (ppm). ^{1}H and ^{13}C NMR are referenced to TMS. ^{7}Li and ^{19}F NMR experiments are referenced to a solution of LiCl/D_2O and CCl_3F, respectively. Coupling constants (J) are reported in Hz. Standard abbreviations are used to indicate multiplicity: s = singlet, d = doublet, t = triplet, and m = multiplet. ^{1}H and ^{13}C peak assignments were performed with the help of additional 2D NMR experiments (^{1}H-^{1}H COSY, ^{1}H−^{1}H NOESY, ^{1}H−^{13}C HSQC, and ^{1}H−^{13}C HMBC). High-resolution mass spectra were recorded at the mass spectrometry service of the Laboratory of Instrumental Techniques (LTI) of the University of Valladolid and the Centros de Apoyo a la Investigación

(CAI) of the University of Alcalá. A MALDI-TOF system (MALDI-TOF) and a Bruker autoflex speed (N_2 laser: 337 nm, pulse energy: 100 μJ, 1 ns; acceleration voltage: 19 kV, reflector positive mode) were used. Trans-2-[3-(4-tert-butylphenyl)-2-methyl-2-propenylidene]malonitrile (DCTB) was used as the matrix. Elemental analysis was obtained using a CHNS-932 Elemental Analyzer at the CAI of the University of Alcalá. In cases where we have been unable to obtain satisfactory elemental analysis, the formulations of the compounds are either supported by X-ray structure determination or high-resolution mass spectroscopy (in addition to NMR spectroscopy).

X-ray Diffraction Studies

Diffraction data were collected using an Oxford Diffraction Supernova diffractometer equipped with an Atlas CCD area detector and a four-circle kappa goniometer. For the data collection, Mo or Cu micro-focused sources with multilayer optics were used. When necessary, crystals were mounted directly from solution using perfluorohydrocarbon oil to prevent atmospheric oxidation, hydrolysis, and solvent loss. Data integration, scaling, and empirical absorption correction were performed using the CrysAlisPro software package. The structure was solved by direct methods and refined by full-matrix-least-squares against F^2 with SHELX in OLEX2. Non-hydrogen atoms were refined anisotropically, and hydrogen atoms were placed at idealized positions and refined using the riding model. Graphics were made with OLEX2 and MERCURY. In the case of **11**, data was collected on a Bruker D8 QUEST diffractometer with an Incoatec IμS Cu microfocus source.

CCDC 1981115-1981137 contain the supplementary crystallographic data for this paper. These data can be obtained free of charge from The Cambridge Crystallographic Data Center.

Synthesis of **2**

^{n}BuLi (8 ml, 20 mmol, 2.5 M in hexane) was dissolved in thf (40 ml). 6-Dibromopyridine (4.74 g, 20 mmol) in thf (28 ml) was added dropwise over 30 min at -78 °C. The resulting dark green

solution was stirred for 70 min at -78 °C. A suspension of $BiCl_3$ (2.1 g, 6.66 mmol) in thf (6 ml) was added dropwise to the lithiated species, and the resulting light green mixture was stirred for 2 h. Subsequently, the resulting white mixture was allowed to reach room temperature. After overnight stirring, all volatiles were removed under vacuum and the resulting white solid residue was extracted with warm toluene (40 ml). The suspension was filtered through Celite to yield a pale-yellow solution, which was concentrated under vacuum until the precipitation of a white solid was observed, which was redissolved by gentle heating. Storage overnight at -24 °C yielded **2** as white blocks suitable for X-ray crystallography. Yield 2.94 g (4.34 mmol, 65%). ^{1}H NMR (298 K, toluene-d_8, 500 MHz): δ = 7.60 (d, J = 6.9 Hz, 3H, H_3 py), 6.78-6.72 (m, 6H, H_4 + H_5 py).^{13}C{^{1}H} NMR (298 K, toluene-d_8, 100.6 MHz): δ =196.2 (br, C_2 py), 132.2 (C_3 py), 145.7 (C_6 py), 138.1 (C_4 py), 126.1 (C_5 py). These resonances were observed and unambiguously assigned through ^{1}H-^{13}C HMBC and ^{1}H-^{13}C HMQC experiments. HR-MS [ESI, positive ion mode ESI-TOF]: m/z for $C_{15}H_9BiBr_3N_3$ [**2**+H]$^+$ calcd: 679.8203. Found: 679.8238 (-5.06 ppm error).

Synthesis of **3**

2-Bromo-6-(trifluoromethyl)pyridine (4.520 g, 20 mmol) was dissolved in diethyl ether (40 ml). To this, ^{n}BuLi (8 ml, 20 mmol, 2.5 M in hexane) was added dropwise over 30 min at -78 °C. The resulting orange solution was stirred for 3 h at -78 °C. A suspension of $BiCl_3$ (2.1 g, 6.66 mmol) in thf (6 ml) was added dropwise to the dark orange lithiated species, and the resulting pale brown mixture was allowed to reach room temperature. After overnight stirring, a dark brown solution with a brown precipitate was observed. All volatiles were removed under vacuum and the resulting solid residue was extracted with warm toluene (40 ml). The suspension was filtered through Celite to yield a brown solution, which was concentrated under vacuum until the precipitation of a white solid was observed, which was redissolved by gentle heating. Storage overnight at -24 °C yielded

3 as white blocks suitable for X-ray crystallography. Yield 3.80 g (5.87 mmol, 88%). ^{1}H NMR (298 K, toluene-d_8, 400 MHz): δ (ppm) = 7.95 (d, J = 7.75 Hz, 3H, H_3 py), 7.03 (t, J = 7.75 Hz, 3H, H_4 py), 6.94 (d, J = 7.75 Hz, 3H, H_5 py). ^{13}C{^{1}H} NMR (298 K, toluene-d_8, 100.5 MHz): δ = 195.7 (br, C_2 py), 150.8 (q, J_{C-F} = 34 Hz, C_6 py), 136.5 (C_4 py), 135.5 (C_3 py), 122.2 (q, J_{C-F} = 272 Hz, C_7 py), 118.5 (q, J_{C-F} = 3 Hz, C_5 py). ^{19}F NMR (298 K, toluene-d_8, 376 MHz): δ = -62.62 (s, 9F, CF_3). Elemental analysis (%) calcd. for **3** ($C_{18}H_9BiF_9N_3$): C 33.4, H 1.4, N 6.5. Found: C 33.2, H 1.6, N 6.4. HR-MS [ESI, positive ion mode ESI-TOF]: m/z for $C_{18}H_9BiF_9N_3$ [**3**+H]$^{+}$ calcd: 648.0529. Found: 648.0532 (-0.35 ppm error).

Synthesis of **4**

2-Bromo-6-(phenyl)pyridine (1.170 g, 5 mmol) was dissolved in thf (20 ml). To this, ^{n}BuLi (2 ml, 5 mmol, 2.5 M in hexane) was added dropwise over 30 min at -78 °C. The resulting red solution was stirred for 1 h at -78 °C. A suspension of $BiCl_3$ (0.525 g, 1.66 mmol) in thf (5 ml) was added dropwise to the dark red lithiated species, and the resulting pale red mixture was allowed to reach room temperature. After overnight stirring, a clear red solution was observed. All volatiles were removed under vacuum, and the resulting solid residue was extracted with warm toluene (15 ml). The suspension was filtered through Celite to yield a red solution, which was concentrated under vacuum until the precipitation of a white solid was observed, which was redissolved by gentle heating. Storage overnight at -24 °C yielded **4** as white needles suitable for X-ray crystallography. Yield 0.663 g (0.99 mmol, 60%). ^{1}H NMR (298 K, toluene-d_8, 500 MHz): δ = 8.09 (d, J = 7.8 Hz, 6H, H_8 Ph), 7.82 (d, J = 7.6 Hz, 3H, H_3 py), 7.27-7.22 (m, 9H, H_5+H_9 py+Ph), 7.21-7.16 (m, 6H, H_4+H_{10} py+Ph). ^{13}C{^{1}H} NMR (298 K, toluene-d_8, 100.6 MHz): δ = 195.42 (C_2 py),159.66 (C_6 py), 139.82 (C_7 Ph),137.08 (C_4 py), 133.14 (C_3 py), 128.97 (C_{10} Ph), 128.78 (C_5 py), 127.26 (C_8 Ph), 118.45 (C_9 Ph). Elemental analysis (%) calcd. for **4** ($C_{33}H_{24}BiN_3$): C 59.0, H 3.6, N 6.3. Found:

C 59.1, H 3.7, N 6.4. HR-MS [ESI, positive ion mode ESI-TOF]: m/z for $C_{18}H_9BiF_9N_3$ [**4**+H]$^+$ calcd: 672.1847. Found: 672.1856 (-1.41 ppm error).

Synthesis of **5**•LiCl•CH_2Cl_2

2-Bromopyridine (1.90 ml, 20 mmol) was dissolved in thf (40 ml). To this ^{n}BuLi (8 ml, 20 mmol, 2.5 M in hexane) was added dropwise over 30 min at -78 °C. The resulting green suspension was stirred for 2.5 h at -78 °C. A suspension of $BiCl_3$ (2.1 g, 6.66 mmol) in thf (6 ml) was added dropwise to lithiated species, and the resulting grey mixture was allowed to reach room temperature. After overnight stirring, a grey solution with a white precipitate was observed. All volatiles were removed under vacuum, and the resulting solid residue was extracted with DCM (40 ml). The suspension was filtered through Celite to yield a red solution, which was concentrated under vacuum, and slow diffusion of n-hexane (20 ml) at -24 °C yielded **5**•LiCl•CH_2Cl_2 as white needles suitable for X-ray crystallography. Yield (calculated as **5**•LiCl•CH_2Cl_2): 2.35 g (4.11 mmol, 61%). ^{1}H NMR (298 K, DMSO-d_6, 500 MHz): δ = 8.60 (m, 3H, H_6 py), 7.80-7.72 (m, 6H, H_4+H_5 py), 7.29 (m, 3H, H_3 py). ^{13}C{^{1}H} NMR (298 K, DMSO-d_6, 100.6 MHz): δ = 194.53 (C_2 py), 152.45 (C_6 py),136.75 (C_4 py), 134.30 (C_5 py), 122.29 (C_3 py). ^{7}Li NMR (298 K, DMSO-d_6, 194.2 MHz): δ = -1.07. ^{7}Li NMR (298 K, $CDCl_3$, 194.2 MHz): δ = 6.25. Elemental analysis (%) calcd. for **5**•LiCl•CH_2Cl_2 ($C_{16}H_{14}BiCl_3LiN_3$): C 33.7, H 2.5, N 7.4. Found: C 34.0, H 2.7, N 8.2. HR-MS [ESI, positive ion mode ESI-TOF]: m/z for $C_{15}H_{12}BiLiN_3$ [**5**+Li]$^+$ calcd: 450.0990. Found: 450.0981 (2.07 ppm error).

Synthesis of **6**•LiBr•CH_2Cl_2

2-Bromo-5-(methyl)pyridine (1.72 g, 10 mmol) was dissolved in thf (20 ml). To this, ^{n}BuLi (4 ml, 10 mmol, 2.5 M in hexane) was added dropwise over 30 min at -78 °C. The resulting red solution was stirred for 2.5 h at -78 °C. A solution of $BiBr_3$ (1.49 g, 3.33 mmol) in thf (5 ml) was

added dropwise to the dark red lithiated species. The resulting pale brown mixture was allowed to reach room temperature. After overnight stirring, a brown solution with a white precipitate was observed. All volatiles were removed under vacuum, and the resulting solid residue was extracted with DCM (20 ml). The suspension was filtered through Celite to yield a brown solution, which was concentrated under vacuum, and slow diffusion of n-hexane (20 ml) at -24 °C yielded **6**•LiBr•CH_2Cl_2 as white needles suitable for X-ray crystallography. Yield (calculated as **6**•LiBr•CH_2Cl_2): 1.59 g (2.42 mmol, 73%). ^{1}H NMR (298 K, DMSO-d_6, 500 MHz): δ = 8.45 (s, 3H, H_6 py), 7.58 (s, 6H, H_3+H_4 py), 2.23 (s, 3H, H_7 Me). $^{13}C\{^1H\}$ NMR (298 K, DMSO-d_6, 100.6 MHz): δ = 189.57 (C_2 py), 152.78 (C_6 py), 137.36 (C_4 py), 133.80 (C_3 py), 131.35 (C_5 py), 18.01 (C_7 Me). ^{7}Li NMR (298 K, DMSO-d_6, 194.2 MHz): δ = -1.16. Elemental analysis (%) calcd. for **6**•LiBr•CH_2Cl_2 ($C_{19}H_{20}BiBrCl_2LiN_3$): 34.7, H 3.1, N 6.4. Found: C 34.0, H 3.2, N 6.5.

Synthesis of **6**•LiCl

2-Bromo-5-(methyl)pyridine (3.44 g, 20 mmol) was dissolved in thf (40 ml). To this, ^{n}BuLi (8 ml, 20 mmol, 2.5 M in hexane) was added dropwise over 30 min at -78 °C. The resulting red solution was stirred for 2.5 h at -78 °C. A suspension of $BiCl_3$ (2.1 g, 6.66 mmol) in thf (6 ml) was added dropwise to the dark red lithiated species. The resulting pale brown mixture was allowed to reach room temperature. After stirring overnight, a brown solution with a white precipitate was observed. All volatiles were removed under vacuum, and the resulting solid residue was extracted with DCM (40 ml). The suspension was filtered through Celite to yield a red solution, which was concentrated under vacuum, and slow diffusion of n-hexane (20 ml) at -24 °C yielded **6**•LiX•CH_2Cl_2 as white needles suitable for X-ray crystallography. Elemental analysis was hampered by salt metathesis resulting in LiX (where X is a mixture of Cl and Br, leading to X = $Cl_{0.6}Br_{0.4}$ as determined from single crystal X-ray crystallography). This problem was avoided in

the preparation of the analogous **6**•LiBr described above. Yield (calculated as **6**•$LiCl_{0.6}Br_{0.4}$•CH_2Cl_2): 2.4 g (3.80 mmol, 57.05%). ^{1}H NMR (298 K, DMSO-d_6, 500 MHz): δ = 8.45 (s, 3H, H_6 py), 7.58 (s, 6H, H_3+H_4 py), 2.23 (s, 3H, H_7 Me).^{13}C{^{1}H} NMR (298 K, DMSO-d_6, 100.6 MHz): δ = 189.57 (C_2 py), 152.78 (C_6 py), 137.36 (C_4 py), 133.80 (C_3 py), 131.35 (C_5 py), 18.01 (C_7 Me). ^{7}Li NMR (298 K, DMSO-d_6, 194.2 MHz): δ = -1.02. ^{7}Li NMR (298 K, $CDCl_3$, 194.2 MHz): δ = 6.21. HR-MS [Maldi, positive ion mode Maldi-TOF]: m/z for $C_{18}H_{18}BiN_3$ [**6**+H]$^+$ calcd: 486.1377. Found: 486.1388 (1.1 ppm error).

Synthesis of **6**•OTf**:**

6•LiX (X = Cl or Br, 0.294 mmol) was dissolved in DCM (10 ml). To this, AgOTf (75.5 mg, 0.294 mmol) was added. The resulting white suspension was stirred for 1 h at rt. The suspension was filtered through Celite to yield a colorless solution which was concentrated under vacuum, and slow diffusion of n-hexane (5 ml) at -24 °C yielded **6**•OTf as white needles suitable for X-ray crystallography. Yield 48 mg (0.082 mmol, 41%). ^{1}H NMR (298 K, $CDCl_3$, 500 MHz): δ = 8.83 (d, J = 2.0 Hz, 3H, H_6 py), 7.72 (d, J = 7.70 Hz, 3H, H_3), 7.51 (dd, J = 2.0/7.70 Hz, 3H, H_4), 2.26 (s, 9H, H_7 Me). ^{13}C{^{1}H} NMR (298 K, $CDCl_3$, 100.6 MHz): δ = 181.4 (C_2 py), 154.7 (C_6 py), 137.8 (C_4 py), 134.7 (C_3 py), 134.1 (C_5 py), 18.7 (C_7 Me). ^{7}Li NMR (298 K, $CDCl_3$, 194.2 MHz): δ = 5.35. ^{19}F NMR (298 K, MeCN-d_3, 376 MHz): δ = -78.02 (s, 3F, OTf^-).

Synthesis of **7**•LiBr•$0.5CH_2Cl_2$

2-Bromo-3-(methyl)pyridine (1.11 ml, 10 mmol) was dissolved in thf (20 ml). To this, ^{n}BuLi (4 ml, 10 mmol, 2.5 M in hexane) was added dropwise (30 min) at -78 °C. The resulting dark red solution was stirred for 2 h at -78 °C. A solution of $BiBr_3$ (1.49 g, 3.33 mmol) in thf (5 ml) was added dropwise to the dark red lithiated species. The resulting brown mixture was allowed to reach room temperature. After overnight stirring, a colorless solution with a white precipitate was

observed. All volatiles were removed under vacuum, and the resulting solid residue was extracted with DCM (20 ml). The suspension was filtered through Celite to yield a red solution, which was concentrated under vacuum, and slow diffusion of n-hexane (20 ml) at -24 °C yielded **7**•LiBr CH_2Cl_2 as white crystals suitable for X-ray crystallography. Yield (calculated as **7**•LiBr•0.5CH_2Cl_2): 1.44 g (2.34 mmol, 75%). ^{1}H NMR (298 K, DMSO-d_6, 500 MHz): δ = 8.29 (d, J = 4.65 Hz, 3H, H_6 py), 7.66 (d, J = 7.5 Hz, 6H, H_4 py), 7.20-7.23 (m, 3H, H_5 py), 2.22 (s, 3H, H_7 Me). ^{13}C{^{1}H} NMR (298 K, DMSO-d_6, 100.6 MHz): δ = 195.92 (C_2 py), 149.71 (C_6 py), 142.89 (C_3 py), 136.39 (C_4 py), 121.99 (C_5 py), 22.56 (C_7 Me). ^{7}Li NMR (298 K, DMSO-d_6, 194.2 MHz): δ = -1.15. Elemental analysis (%) Calcd. for **7**•LiBr•0.5CH_2Cl_2 ($C_{18.5}H_{19}BiBrClLiN_3$): C 36.2, H 3.1, N 6.8. Found C 36.5, H 3.3, N 7.3.

Synthesis of **7**•LiX

2-Bromo-3-(methyl)pyridine (2.22 ml, 20 mmol) was dissolved in thf (30 ml). To this, ^{n}BuLi (8 ml, 20 mmol, 2.5 M in hexane) was added dropwise over 30 min at -78 °C. The resulting dark red solution was stirred for 2 h at -78 °C. A suspension of $BiCl_3$ (2.1 g, 6.66 mmol) in thf (6 ml) was added dropwise to the dark red lithiated species. The resulting brown mixture was allowed to reach room temperature. After overnight stirring, a colorless solution with a white precipitate was observed. All volatiles were removed under vacuum, and the resulting solid residue was extracted with DCM (40 ml). The suspension was filtered through Celite to yield a red solution, which was concentrated under vacuum, and slow diffusion of n-hexane (20 ml) at -24 °C yielded 7•$LiCl_{0.7}Br_{0.3}$•CH_2Cl_2 as white needles suitable for X-ray crystallography. When the samples were left under persistent vacuum, an amorphous material that was found to contain no CH_2Cl_2 solvation was obtained, corresponding to **7**•$LiCl_{0.7}Br_{0.3}$. Yield (calculated as **7**•$LiCl_{0.7}Br_{0.3}$): 1.78 g (3.28 mmol, 49.2 %). ^{1}H NMR (298 K, DMSO-d_6, 500 MHz): δ = 8.29 (d, J = 4.65 Hz, 3H, H_6 py), 7.66

(d, J = 7.5 Hz, 6H, H_4 py), 7.20-7.23 (m, 3H, H_5 py), 2.22 (s, 3H, H_7 Me). $^{13}C\{^1H\}$ NMR (298 K, DMSO-d_6, 100.6 MHz): δ = 195.92(C_2 py), 149.71 (C_6 py), 142.89 (C_3 py), 136.39 (C_4 py), 121.99 (C_5 py), 22.56 (C_7 Me). ^{7}Li NMR (298 K, DMSO-d_6, 194.2 MHz): δ = -0.91. ^{7}Li NMR (298 K, $CDCl_3$, 194.2 MHz): δ = 6.73. HR-MS [Maldi, positive ion mode Maldi-TOF]: m/z for $C_{18}H_{18}BiLiN_3$ [**7**+Li]$^+$ calcd: 492.1460. Found: 492.1485 (2.5 ppm error). HR-MS [Maldi, positive ion mode Maldi-TOF]: m/z for $C_{18}H_{18}BiN_3$ [**7**+H]$^+$ calcd: 486.1377. Found: 486.1405 (2.8 ppm error). We found that when samples were left to crystallize for long periods, salt metathesis can occur, leading to the formation of crystals of 7LiX (X = Cl, Br) containing variable amounts of LiBr. When this happens, bulk samples of pure **7**•LiCl can be obtained by treatment with an excess of tetrabutyl ammonium chloride (TBACl) as follows. Typically, 100 mg of LiX and TBACl (415 mg, 3.79 mmol) were dissolved in DCM (4 ml). After overnight stirring, the colorless solution was concentrated under vacuum, and slow diffusion of n-hexane (3 ml) at -24 °C yielded **7**•LiCl•CH_2Cl_2 as colorless crystals suitable for X-ray crystallography. Yield (calculated as **7**•LiCl•CH_2Cl_2): 62.8 mg (0.11 mmol, 58%). Elemental analysis (%) Calcd. for **7**•LiCl ($C_{18}H_{18}BiClLiN_3$): C 41.0, H 3.4, N 8.00. Found: C 41.8, H 4.0, N 8.1.

Decoordination of LiX from ligands **5** and **6**

A suspension of **5**•LiX or **6**•LiX (0.20 mmol) in toluene (10 ml) was extracted with water (3 x 2 ml). The extract was dried over anhydrous magnesium sulphate, then filtered through Celite. The solvent was removed by evaporation under reduced pressure to give a white oil, which yielded crystalline samples of halide-free **5** and **6** as colorless needles overnight at -24 °C. The absence of LiX in the samples was verified by ^{7}Li NMR spectroscopy. Compound **5**. Yield: 65.7 mg (0.148 mmol, 72%). ^{1}H NMR (298 K, $CDCl_3$, 500 MHz): δ = 8.68 (m, 3H, H_6 py), 7.73 (m, 6H, H_5 py), 7.65 (m, 3H, H_4 py), 8.21 (m, 3H, H_3 py). $^{13}C\{^1H\}$ NMR (298 K, $CDCl_3$, 100.6 MHz): δ = 194.3

(C_2 py), 152.9 (C_6 py),137.2 (C_4 py), 134.0 (C_5 py), 122.3 (C_3 py). HR-MS [Maldi, positive ion mode Maldi-TOF]: m/z for $C_{15}H_{12}BiN_3$ $[M+H]^+$ calcd: 444.0908. Found: 444.0919 (1.1 ppm error). Compound **6**. Yield 59.2 mg (0.12 mmol, 64%). ^{1}H NMR (298 K, $CDCl_3$, 500 MHz): δ = 8.51 (br, 3H, H_6 py), 7.58 (d, J = 7.70 Hz, 3H, H_3), 7.43 (dd, J = 2.0/7.70 Hz, 3H, H_4), 2.26 (s, 9H, H_7 Me). HR-MS [Maldi, positive ion mode Maldi-TOF]: m/z for $C_{18}H_{18}BiN_3$ $[M+H]^+$ calcd: 486.1377. Found: 486.1388 (1.1 ppm error).

Synthesis of silver complexes **8**•X (X = OTf, BF_4, PF_6)

0.144 mmol of the corresponding silver salt (36.99 mg, 28.03 mg, and 36.40 mg for AgOTf, $AgBF_4$, and $AgPF_6$, respectively) were dissolved in MeCN (5 mL) in the dark. After stirring the mixture for 1 h, all volatiles were removed under vacuum, and the resulting white solid was dissolved in thf (5 ml). Bi(6-Me-2-py)$_3$ (**1**) (70 mg, 0.144 mmol) in thf (3 ml) was added to give a white precipitate. The solvents were evaporated, the residue was dissolved in MeCN (5 mL), and the solution was concentrated until the formation of a white precipitate was observed, which was redissolved by gentle heating. Storage at -24 °C yielded **8**•OTf•CH_3CN, **8**•BF_4, and **8**•PF_6•2CH_3CN as colorless crystals suitable for X-ray crystallography. Crystalline yield (calculated for all crystals): 62.6 mg (0.076 mmol, 53%), 60.5 mg (0.084 mmol, 60%), and 58.5 mg (0.068 mmol, 47%), respectively. The crystals were found to be very unstable towards light and moisture, resulting in loss of crystallinity and the rapid formation of a black amorphous solid, which hampered elemental analysis. ^{1}H and ^{13}C NMR spectra for **8**•X were found to be identical within the experimental error. ^{1}H NMR (298 K, MeCN-d_3, 500 MHz): δ = 7.83 (d, J = 7.40 Hz, 3H, H_3 py), 7.76 (t, J = 7.40 Hz, 3H, H_4 py), 7.32 (d, J = 7.40 Hz, 3H, H_5 py), 2.74 (s, 9H, H_7 Me). ^{13}C{^{1}H} NMR (298 K, MeCN-d_3, 100.6 MHz): δ = 194.2 (br, C_2 py), 161.9 (C_6 py), 137.9 (C_4 py), 133.5 (C_3 py), 124.0 (C_5 py), 25.8 (C_7 Me). **8**•OTf: ^{19}F NMR (298 K, MeCN-d_3, 376 MHz): δ = -

79.25 (s, 3F, OTf^-). **8**•BF_4: ^{19}F NMR (298 K, MeCN-d_3, 376 MHz): δ = -151.71 (br, $^{10}BF_4^-$), -151.76 (br, $^{11}BF_4^-$). **8**•PF_6: ^{19}F NMR (298 K, MeCN-d_3, 376 MHz): δ = -72.8 (d, 6F, J_{PF} = 707 Hz, PF_6^-). HR-MS [Maldi, positive ion mode Maldi-TOF]: m/z for $C_{18}H_{18}AgBiN_3$ [**8**-CH_3N]$^+$ calcd: 592.035. Found: 592.0349 (-0.1 ppm error).

Synthesis of **9**•BF_4

$AgBF_4$ (14.49 mg, 0.074 mmol) was dissolved in MeCN (2 ml) in the dark. After 30 min of stirring, all volatiles were removed under vacuum, and the resulting white solid was redissolved in thf (2 ml). Then, Bi(6-Ph-2-py)$_3$ (**4**) (50 mg, 0.074 mmol) in thf (2 ml) was added to give a white precipitate. Subsequently, the solvents were evaporated and the residue was redissolved in MeCN (5 ml). The colorless solution was concentrated under vacuum until the precipitation of a white precipitate was observed. Storage at -24 °C yielded **9**•BF_4 as colorless crystals suitable for X-ray crystallography. The product was isolated by filtration. Yield 45 mg (0.049 mmol, 66%). Similarly to **8**•X**,** the crystals of **9**•BF_4 were found to be very unstable towards light and moisture, resulting in rapid loss of crystallinity and formation of a black amorphous solid, which hampered elemental analysis. ^1H NMR (298 K, MeCN-d_3, 500 MHz): δ = 8.00-7.96 (m, 6H, H_3+H_4 py), 7.71 (m, 3H, H_5 py), 7.59 (d, J = 7.10 Hz, 6H, H_8 Ph), 7.39 (t, J = 7.10 Hz, 6H, H_{10} Ph), 7.31 (t, J = 7.10 Hz, 6H, H_9 Ph). $^{13}C\{^1H\}$ NMR (298 K, MeCN-d_3, 100.6 MHz): δ =198.3 (br, C_2 py), 163.19 (C_6 py), 141.9 (C_7 Ph), 139.3 (C_4 py), 135.6 (C_3 py), 130.2 (C_{10} Ph), 129.4 (C_9 Ph), 128 (C_8 Ph), 123.2 (C_5 Ph). ^{19}F NMR (298 K, MeCN-d_3, 376 MHz): δ = -151.97 (s, $^{10}BF_4^-$), -152.03 (s, $^{11}BF_4^-$). HR-MS [Maldi, positive ion mode Maldi-TOF]: m/z for $C_{33}H_{24}AgBiN_3$ [**9**-CH_3CN]$^+$ calcd: 778.0820. Found: 778.0824 (0.4 ppm error).

Synthesis of **10**

Bi(6-Me-2-py)$_3$ (150 mg, 0.30 mmol) was dissolved in MeCN (2 ml)/THF (2 ml). To this solution, [Cu(MeCN)$_4$]BF$_4$ (97.1 mg, 0.30 mmol) was added. The resulting pale-yellow solution was stirred for 24 h at room temperature. The solution was filtered through Celite to yield a red solution, which was concentrated under vacuum. Storage at -24 °C for several weeks yielded **10** as a few orange crystals suitable for X-ray crystallography, along with the red crystals of [Cu(Me-bpy)$_2$]BF$_4$ (Me-bpy = 6,6'-dimethyl-2,2'-bipyridyl; see SI) and a black precipitate.

Synthesis of **11a•**CH$_3$CN**;**

Bi(6-Me-2-py)$_3$ (**1**) (100 mg, 0.20 mmol) was dissolved in MeCN (5 ml). To this solution, CuCl$_2$ (27.7 mg, 0.20 mmol) was added. The resulting red solution was stirred for 15 min at rt. The solution was filtered through Celite to yield a red solution, which was concentrated under vacuum, and slow diffusion of diethyl ether (5 ml) at -24 °C yielded **11a•**CH$_3$CN as red pale crystals suitable for X-ray crystallography. **11a•**CH$_3$CN Yield (calculated as **11a•**CH$_3$CN): 48 mg (0.078 mmol, 40%). ^{1}H NMR (298 K, MeCN-d$_3$, 500 MHz): δ = 8.20 (d, J = 7.70 Hz, 2H, H$_3$ py), 7.91 (t, J = 7.70 Hz, 2H, H$_4$ py), 7.32 (d, J = 7.70 Hz, 2H, H$_5$ py), 2.79 (s, 6H, H$_7$ Me). ^{13}C{^{1}H} NMR (298 K, MeCN-d$_3$, 100.6 MHz): δ = 216.6 (br, C$_2$ py), 163.5 (C$_6$ py), 139.0 (C$_4$ py), 135.4 (C$_3$ py), 124.4 (C$_5$ py), 26.0 (C$_7$ Me). Elemental analysis (%) calcd. for **11a•**CH$_3$CN (C$_{16}$H$_{18}$BiCl$_2$CuN$_4$): C 31.5, H 3.0, N 9.2. Found C 31.0, H 2.9, N 8.6. HR-MS [Maldi, positive ion mode Maldi-TOF]: m/z for C$_{12}$H$_{12}$BiClN$_2$Cu [M-Cl-CH$_3$CN]$^+$ calcd: 490.9783. Found: 490.9762 (-2.1 ppm error).

Synthesis of **11b**

Bi(6-CF$_3$-2-py)$_3$ (**3**) (200 mg, 0.30 mmol) was dissolved in MeCN (5 ml). To this solution, CuCl$_2$ (124.6 mg, 0.90 mmol) was added. The resulting pale-yellow solution was stirred overnight at rt. The solution was filtered through Celite to yield a yellow solution, which was concentrated under vacuum, and slow diffusion of diethyl ether (5 ml) at -24 °C yielded **11b** as yellow blocks suitable

for X-ray crystallography. Samples were found to contain variable amounts of the ligand Bi(6-CF_3-2-py)$_3$ as demonstrated by crystallography and NMR studies. For this reason, a specific yield cannot be provided. ^{1}H NMR (298 K, MeCN-d_3, 500 MHz): δ = 8.47 (d, J = 7.80 Hz, 2H, H_3 py), 8.20 (t, J = 7.80 Hz, 2H, H_4 py), 7.76 (d, J = 7.80 Hz, 2H, H_5 py).

Synthesis of **11c•**CH_2Cl_2

Bi(6-Me-2-py)$_3$ (100 mg, 0.20 mmol) was dissolved in MeCN (5 ml). To this solution, $CuBr_2$ (46 mg, 0.20 mmol) was added. The resulting red solution was stirred for 15 min at rt. The solution was filtered through Celite to yield a red solution, which was concentrated under vacuum. Slow diffusion of diethyl ether (5 ml) at -24 °C yielded **11c•** CH_2Cl_2 as pale red crystals suitable for X-ray crystallography. Yield (calculated as **11c•**CH_2Cl_2) 36.8 mg (0.049 mmol, 24%). ^{1}H NMR (298 K, MeCN-d_3, 500 MHz): δ = 8.35 (d, J = 7.80 Hz, 2H, H_3 py), 7.88 (t, J = 7.80 Hz, 2H, H_4 py), 7.35 (d, J = 7.80 Hz, 2H, H_5 py), 2.79 (s, 6H, H_7 Me). ^{13}C{^{1}H} NMR (298 K, MeCN-d_3, 100.6 MHz): δ = 212.2 (br, C_2 py), 163.6 (C_6 py), 139.0 (C_4 py), 137.0 (C_3 py), 124.5 (C_5 py), 25.9 (C_7 Me). HR-MS [Maldi, positive ion mode Maldi-TOF]: m/z for $C_{12}H_{12}BiBrN_2Cu$ $[M\text{-}Br\text{-}CH_3CN]^+$ calcd: 536.9259. Found: 536.926 (0.1 ppm error).

Synthesis of **12**

Inside a N_2 filled glovebox, a Schlenk tube was charged with Bi(6-Me-2-py)$_3$ (**1**) (200 mg, 0.41 mmol) and $FeCl_2$ (52 mg, 0.41 mmol) and transferred to a Schlenk line. 20 ml of thf was added. The resulting pale orange solution was stirred overnight at room temperature. An orange solution with a small amount of brown precipitate formed overnight and was removed by filtration. The clear orange filtrate was concentrated under vacuum to approximately 5 ml. Storage at -20 °C yielded a few yellow crystals suitable for X-ray crystallography.

Synthesis of **13**

FeI_2 (92.8 mg, 0.30 mmol) was dissolved in thf (5 ml). To this black solution, $Bi(6\text{-Me-2-py})_3$ (**1**) (150 mg, 0.30 mmol) was added. The resulting brown suspension was stirred overnight at room temperature. All volatiles were removed under vacuum, and the resulting solid residue was redissolved in MeCN (5 ml). This suspension was filtered through Celite, which was redissolved by gentle heating. Storage overnight at -24 °C yielded **13** as a few yellow crystals suitable for X-ray crystallography.

Synthesis of **14**•OTf

$(PPh)_3AuOTf$ (15.9 mg, 0.032 mmol) and $Bi(6\text{-Me-2-py})_3$ was dissolved in acetone (2 ml). Then, a solution of $Bi(6\text{-Me-2-py})_3$ (**1**) (20 mg, 0.032 mmol) was added. After stirring for 30 min at room temperature, the colorless solution was concentrated under vacuum. Storage at -24 °C yielded **14** as a few colorless blocks suitable for X-ray crystallography.

ASSOCIATED CONTENT

Supporting Information.

The following files are available free of charge: NMR spectra, additional X-ray structures, details and information, and HR-MS data (PDF).

AUTHOR INFORMATION

Corresponding Author

*Email: celedonio.alvarez@uva.es

*E-mail: raul.garcia.rodriguez@uva.es

Author Contributions

The manuscript was written through contributions of all authors.

ACKNOWLEDGMENT

We thank The Leverhulme Trust (R.G.-R., DSW) (RPG-2017-146), the Cambridge Trust (Vice Chancellor Scholarship for AJP) and The Spanish Ministry of Science, Innovation and Universities (MCIU) (project numbers PGC2018-096880-A-I00, MCIU/AEI/FEDER, UE and PGC2018-099470-B-I00, MCIU/AEI/FEDER, UE) for funding. R.G.-R. acknowledges the Spanish MINECO/AEI and the European Union (ESF) for a Ramon y Cajal contract (RYC-2015−19035). We thank Alberto Diez-Varga for help in collecting some of the mass data.

REFERENCES

(1) Moberg, C. C_3 Symmetry in Asymmetric Catalysis and Chiral Recognition. *Angew. Chemie Int. Ed.* **1998**, *37* (3), 248–268.
(2) Trofimenko, S. Recent Advances in Poly(Pyrazolyl)Borate (Scorpionate) Chemistry. *Chem. Rev.* **1993**, *93* (3), 943–980.
(3) Szczepura, L. F.; Witham, L. M.; Takeuchi, K. J. Tris(2-Pyridyl) Tripod Ligands. *Coord. Chem. Rev.* **1998**, *174* (1), 5–32.
(4) Maleckis, A.; Kampf, J. W.; Sanford, M. S. A Detailed Study of Acetate-Assisted C–H Activation at Palladium(IV) Centers. *J. Am. Chem. Soc.* **2013**, *135* (17), 6618–6625.
(5) Walden, A. G.; Miller, A. J. M. Rapid Water Oxidation Electrocatalysis by a Ruthenium Complex of the Tripodal Ligand Tris(2-Pyridyl)Phosphine Oxide. *Chem. Sci.* **2015**, *6* (4), 2405–2410.
(6) Camasso, N. M.; Sanford, M. S. Design, Synthesis, and Carbon-Heteroatom Coupling Reactions of Organometallic Nickel(IV) Complexes. *Science* **2015**, *347* (6227), 1218–1220.
(7) Martínez-García, H.; Morales, D.; Pérez, J.; Puerto, M.; del Río, I. Interaction between Anions and Cationic Metal Complexes Containing Tridentate Ligands with *Exo*-C-H Groups: Complex Stability and Hydrogen Bonding. *Chem. - A Eur. J.* **2014**, *20* (19), 5821–5834.
(8) Reichart, F.; Kischel, M.; Zeckert, K. Lanthanide(II) Complexes of a Dual Functional Tris(2-Pyridyl)Stannate Derivative. *Chem. - A Eur. J.* **2009**, *15* (39), 10018–10020.
(9) García, F.; Hopkins, A. D.; Humphrey, S. M.; McPartlin, M.; Rogers, M. C.; Wright, D. S. The First Example of a Si-Bridged Tris(Pyridyl) Ligand; Synthesis and Structure of $[MeSi(2\text{-}C_5H_4N)_3LiX]$ (X = 0.2Br, 0.8Cl). *Dalt. Trans.* **2004**, No. 3, 361–362.
(10) Morales, D.; Pérez, J.; Riera, L.; Riera, V.; Miguel, D. Molybdenum and Tungsten Tricarbonyl Complexes with the Tripodal Ligands $[^nBuSn(2\text{-Pyridyl})_3]$ and $[RSn(Methylthiomethyl)_3]$. *Organometallics* **2001**, *20* (22), 4517–4523.
(11) García-Rodríguez, R.; Kopf, S.; Wright, D. S. Modifying the Donor Properties of Tris(Pyridyl)Aluminates in Lanthanide(II) Sandwich Compounds. *Dalt. Trans.* **2018**, *47* (7), 2232–2239.
(12) Zeckert, K. Pyridyl Compounds of Heavier Group 13 and 14 Elements as Ligands for

Lanthanide Metals. *Organometallics* **2013**, *32* (5), 1387–1393.
(13) Beswick, M. A.; Davies, M. K.; Raithby, P. R.; Steiner, A.; Wright, D. S. Synthesis and Structure of [Pb(2-Py)$_3$Li·THF], Containing a Low-Valent Group 14 Tris(Pyridyl) Ligand (2-Py = 2-Pyridyl). *Organometallics* **1997**, *16* (6), 1109–1110.
(14) Alvarez, C. S.; García, F.; Humphrey, S. M.; Hopkins, A. D.; Kowenicki, R. A.; McPartlin, M.; Layfield, R. A.; Raja, R.; Rogers, M. C.; Woods, A. D.; Wright, D. S. Highly Selective Epoxidation of Styrene Using a Transition Metal–Aluminium(III) Complex Containing the [MeAl(2-Py)$_3$]$^-$ Anion (2-Py = 2-Pyridyl). *Chem. Commun.* **2005**, *0* (2), 198–200.
(15) Zeckert, K.; Griebel, J.; Kirmse, R.; Weiß, M.; Denecke, R. Versatile Reactivity of a Lithium Tris(Aryl)Plumbate(II) towards Organolanthanoid Compounds: Stable Lead-Lanthanoid-Metal Bonds or Redox Processes. *Chem. - A Eur. J.* **2013**, *19* (24), 7718–7722.
(16) Schrader, I.; Zeckert, K.; Zahn, S. Dilithium Hexaorganostannate(IV) Compounds. *Angew. Chemie - Int. Ed.* **2014**, *53* (50), 13698–13700.
(17) Plajer, A. J.; Colebatch, A. L.; Enders, M.; García-Romero, Á.; Bond, A. D.; García-Rodríguez, R.; Wright, D. S. The Coordination Chemistry of the Neutral Tris-2-Pyridyl Silicon Ligand [PhSi(6-Me-2-Py)$_3$]. *Dalt. Trans.* **2018**, *47* (20), 7036–7043.
(18) Zeckert, K.; Zahn, S.; Kirchner, B. Tin-Lanthanoid Donor-Acceptor Bonds. *Chem. Commun.* **2010**, *46* (15), 2638–2640.
(19) García-Rodríguez, R.; Bullock, T. H.; McPartlin, M.; Wright, D. S. Synthesis and Structures of Tris(2-Pyridyl)Aluminate Sandwich Compounds [{RAl(2-Py′)$_2$}$_2$M] (Py′ = 2-Pyridyl, M = Ca, Mn, Fe). *Dalt. Trans.* **2014**, *43* (37), 14045–14053.
(20) García-Rodríguez, R.; Simmonds, H. R.; Wright, D. S. Formation of a Heterometallic Al^{III}/Sm^{III} Complex Involving a Novel [EtAl(2-Py)$_2$O]$^{2-}$ Ligand (2-Py = 2-Pyridyl). *Organometallics* **2014**, *33* (24), 7113–7117.
(21) Matson, B. D.; Peters, J. C. Fe-Mediated HER vs N_2RR: Exploring Factors That Contribute to Selectivity in $P_3^EFe(N_2)$ (E = B, Si, C) Catalyst Model Systems. *ACS Catal.* **2018**, *8* (2), 1448–1455.
(22) Thomas, J. C.; Peters, J. C. Zwitterionic and Cationic Bis(Phosphine) Platinum(II) Complexes: Structural, Electronic, and Mechanistic Comparisons Relevant to Ligand Exchange and Benzene C-H Activation Processes. *J. Am. Chem. Soc.* **2003**, *125* (29), 8870–8888.
(23) Del Castillo, T. J.; Thompson, N. B.; Peters, J. C. A Synthetic Single-Site Fe Nitrogenase: High Turnover, Freeze-Quench ^{57}Fe Mössbauer Data, and a Hydride Resting State. *J. Am. Chem. Soc.* **2016**, *138* (16), 5341–5350.
(24) Simmonds, H. R.; Wright, D. S. Main Group Pyridyl-Based Ligands; Strategies to Mixed Metal Complexes. *Chem. Commun.* **2012**, *48* (69), 8617.
(25) Plajer, A. J.; Colebatch, A. L.; Rizzuto, F. J.; Pröhm, P.; Bond, A. D.; García-Rodríguez, R.; Wright, D. S. How Changing the Bridgehead Can Affect the Properties of Tripodal Ligands. *Angew. Chemie Int. Ed.* **2018**, *57* (22), 6648–6652.
(26) Cui, C.; Lalancette, R. A.; Jäkle, F. The Elusive Tripodal Tris(2-Pyridyl)Borate Ligand: A Strongly Coordinating Tetraarylborate. *Chem. Commun.* **2012**, *48* (55), 6930–6932.
(27) Cui, C.; Shipman, P. R.; Lalancette, R. A.; Jäkle, F. Tris(2-Pyridylborate) (Tpyb) Metal Complexes: Synthesis, Characterization, and Formation of Extrinsically Porous Materials with Large Cylindrical Channels. *Inorg. Chem.* **2013**, *52* (16), 9440–9448.
(28) Jeong, S. Y.; Lalancette, R. A.; Lin, H.; Lupinska, P.; Shipman, P. O.; John, A.; Sheridan, J. B.; Jäkle, F. "third-Generation"-Type Functional Tris(2-Pyridyl)Borate Ligands and

Their Transition-Metal Complexes. *Inorg. Chem.* **2016**, *55* (7), 3605–3615.
(29) García-Rodríguez, R.; Wright, D. S. Steric Effects on the Structures, Reactivity, and Coordination Chemistry of Tris(2-Pyridyl)Aluminates. *Chem. - A Eur. J.* **2015**, *21* (42), 14949–14957.
(30) Plajer, A. J.; Kopf, S.; Colebatch, A. L.; Bond, A. D.; Wright, D. S.; García-Rodríguez, R. Deprotonation, Insertion and Isomerisation in the Post-Functionalisation of Tris-Pyridyl Aluminates. *Dalt. Trans.* **2019**, *48* (17), 5692–5697.
(31) García-Romero, Á.; Plajer, A. J.; Álvarez-Miguel, L.; Bond, A. D.; Wright, D. S.; García-Rodríguez, R. Postfunctionalization of Tris(Pyridyl) Aluminate Ligands: Chirality, Coordination, and Supramolecular Chemistry. *Chem. – A Eur. J.* **2018**, *24* (64), 17019–17026.
(32) García-Rodríguez, R.; Wright, D. S. Direct Synthesis of the Janus-Head Ligand (^{Me}Py)$_3$Sn-Sn(^{Me}Py)$_3$ Using an Unusual Pyridyl-Transfer Reaction (^{Me}Py = 6-Methyl-2-Pyridyl). *Dalt. Trans.* **2014**, *43* (39), 14529–14532.
(33) García, F.; Hopkins, A. D.; Kowenicki, R. A.; McPartlin, M.; Rogers, M. C.; Wright, D. S. Synthesis of the [MeAl(2-Py)$_3$]$^-$ Anion and Its Application as a Stable and Mild Pyridyl-Transfer Reagent (2-Py = 2-Pyridyl). *Organometallics* **2004**, *23* (16), 3884–3890.
(34) García-Rodríguez, R.; Hanf, S.; Bond, A. D.; Wright, D. S. A Non-Chiral Lithium Aluminate Reagent for the Determination of Enantiomeric Excess of Chiral Alcohols. *Chem. Commun.* **2017**, *53* (7), 1225–1228.
(35) Szczepura, L. F.; Witham, L. M.; Takeuchi, K. J. Tris(2-Pyridyl) Tripod Ligands. *Coord. Chem. Rev.* **1998**, *174* (1), 5–32.
(36) Hanf, S.; García-Rodríguez, R.; Bond, A. D.; Hey-Hawkins, E.; Wright, D. S. Sterically-Constrained Tripodal Phosphorus-Bridged Tris-Pyridyl Ligands. *Dalt. Trans.* **2016**, *45* (1), 276–283.
(37) Gneuß, T.; Leitl, M. J.; Finger, L. H.; Rau, N.; Yersin, H.; Sundermeyer, J. A New Class of Luminescent Cu(I) Complexes with Tripodal Ligands-TADF Emitters for the Yellow to Red Color Range. *Dalt. Trans.* **2015**, *44* (18), 8506–8520.
(38) Ni, J.; Wei, K. J.; Min, Y.; Chen, Y.; Zhan, S.; Li, D.; Liu, Y. Copper(I) Coordination Polymers of 2,2′-Dipyridylamine Derivatives: Syntheses, Structures, and Luminescence. *Dalt. Trans.* **2012**, *41* (17), 5280–5293.
(39) Pérez, J.; Morales, D.; García-Escudero, L. A.; Martínez-García, H.; Miguel, D.; Bernad, P. Synthesis of New Copper(I) Complexes with Tris(2-Pyridyl) Ligands. Applications to Carbene and Nitrene Transfer Reactions. *J. Chem. Soc. Dalt. Trans.* **2009**, *1* (2), 375–382.
(40) Yang, W.; Schmider, H.; Wu, Q.; Zhang, Y. S.; Wang, S. Syntheses, Structures, and Fluxionality of Blue Luminescent Zinc(II) Complexes: Zn(2,2',2-Tpa)Cl$_2$, Zn(2,2',2-Tpa)$_2$(O$_2$CCF$_3$)$_2$, and Zn(2,2',3-Tpa)$_4$(O$_2$CCF$_3$)$_2$ (Tpa = Tripyridylamine). *Inorg. Chem.* **2000**, *39* (11), 2397–2404.
(41) Richard Keene, F.; Stephenson, P. J.; Snow, M. R.; Tiekink, E. R. T. Ruthenium(II) Complexes of the C$_{3v}$ Ligands Tris(2-Pyridyl)Amine, Tris(2-Pyridyl)Methane, and Tris(2-Pyridyl)Phosphine. 1. Synthesis and X-Ray Structural Studies of the Bis(Ligand) Complexes. *Inorg. Chem.* **1988**, *27* (12), 2040–2045.
(42) Hanf, S.; García-Rodríguez, R.; Feldmann, S.; Bond, A. D.; Hey-Hawkins, E.; Wright, D. S. Multidentate 2-Pyridyl-Phosphine Ligands-towards Ligand Tuning and Chirality. *Dalt. Trans.* **2017**, *46* (3), 814–824.
(43) Steiner, A.; Stalke, D. Substituent-Controlled Reactions of Iminophosphoranes with

Methyllithium. *Angew. Chemie Int. Ed. English* **1995**, *34* (16), 1752–1755.
(44) Steiner, A.; Stalke, D. Bis(2-Pyridyl)Phosphides and -Arsenides of Group 13 Metals: Substituent-Separated Contact Ion Pairs. *Organometallics* **1995**, *14* (5), 2422–2429.
(45) Artem'ev, A. V.; Doronina, E. P.; Rakhmanova, M. I.; Sutyrina, A. O.; Bagryanskaya, I. Y.; Tolstoy, P. M.; Gushchin, A. L.; Mazur, A. S.; Gusarova, N. K.; Trofimov, B. A. Luminescent Cu^{I} Thiocyanate Complexes Based on Tris(2-Pyridyl)Phosphine and Its Oxide: From Mono-, Di- and Trinuclear Species to Coordination Polymers. *New J. Chem.* **2016**, *40* (12), 10028–10040.
(46) Suter, R.; Sinclair, H.; Burford, N.; McDonald, R.; Ferguson, M. J.; Schrader, E. Tris(2-Pyridyl)Phosphine as a Versatile Ligand for Pnictogen Acceptors. *Dalt. Trans.* **2017**, *46* (24), 7681–7685.
(47) Dedert, P. L.; Thompson, J. S.; Ibers, J. A.; Marks, T. J. Metal Ion Binding Sites Composed of Multiple Nitrogenous Heterocycles. Synthesis and Spectral and Structural Study of Bis(2,2′,2″-Tripyridylamine)Copper(II) Bis(Trifluoromethanesulfonate) and Its Bis(Acetonitrile) Adduct. *Inorg. Chem.* **1982**, *21* (3), 969–977.
(48) Dedert, P. L.; Sorrell, T.; Marks, T. J.; Ibers, J. A. Oxygenation of [Tris(2-Pyridyl)Amine](Trifluoromethanesulfonato)Copper(I) in Nonaqueous Solvents. Synthesis and Structural Characterization of the Cubane-like Cluster $[Cu_4(OH)_4(SO_3CF_3)_2[N(C_5H_4N)_3]_4][SO_3CF_3]_2 \cdot C_3H_6O$. *Inorg. Chem.* **1982**, *21* (9), 3506–3517.
(49) Ross, S.; Weyhermüller, T.; Bill, E.; Wieghardt, K.; Chaudhuri, P. Tris(Pyridinealdoximato)Metal Complexes as Ligands for the Synthesis of Asymmetric Heterodinuclear $Cr^{III}M$ Species [M = Zn(II), Cu(II), Ni(II), Fe(II), Mn(II), Cr(II), Co(III)]: A Magneto-Structural Study. *Inorg. Chem.* **2001**, *40* (26), 6656–6665.
(50) Suzuki, H; Matano, Y., eds. Chapter 1. Introduction in *Organobismuth Chemistry*; Elsevier Science, Amsterdan, **2001**; pp 1-20.
(51) Stephens, L. J.; Munuganti, S.; Duffin, R. N.; Werrett, M. V.; Andrews, P. C. Is Bismuth Really the "Green" Metal? Exploring the Antimicrobial Activity and Cytotoxicity of Organobismuth Thiolate Complexes. *Inorg. Chem.* **2020**, 59 (6), 3494-3508.
(52) Mohan, R. Green Bismuth. *Nat. Chem.* **2010**, *2* (4), 336.
(53) Lichtenberg, C.; Pan, F.; Spaniol, T. P.; Englert, U.; Okuda, J. The Bis(Allyl)Bismuth Cation: A Reagent for Direct Allyl Transfer by Lewis Acid Activation and Controlled Radical Polymerization. *Angew. Chemie - Int. Ed.* **2012**, *51* (52), 13011–13015.
(54) Chitnis, S. S.; Robertson, A. P. M.; Burford, N.; Patrick, B. O.; McDonald, R.; Ferguson, M. J. Bipyridine Complexes of E^{3+} (E = P, As, Sb, Bi): Strong Lewis Acids, Sources of $E(OTf)_3$ and Synthons for E^{I} and E^{V} Cations. *Chem. Sci.* **2015**, *6* (11), 6545–6555.
(55) Solyntjes, S.; Neumann, B.; Stammler, H. G.; Ignat'ev, N.; Hoge, B. Bismuth Perfluoroalkylphosphinates: New Catalysts for Application in Organic Syntheses. *Chem. - A Eur. J.* **2017**, *23* (7), 1568–1575.
(56) Wang, F.; Planas, O.; Cornella, J. Bi(I)-Catalyzed Transfer-Hydrogenation with Ammonia-Borane. *J. Am. Chem. Soc.* **2019**, *141* (10), 4235–4240.
(57) Yin, S. F.; Maruyama, J.; Yamashita, T.; Shimada, S. Efficient Fixation of Carbon Dioxide by Hypervalent Organobismuth Oxide, Hydroxide, and Alkoxide. *Angew. Chemie - Int. Ed.* **2008**, *47* (35), 6590–6593.
(58) Casely, I. J.; Ziller, J. W.; Fang, M.; Furche, F.; Evans, W. J. Facile Bismuth-Oxygen Bond Cleavage, C-H Activation, and Formation of a Monodentate Carbon-Bound Oxyaryl

Dianion, $(C_6H_2tBu2\text{-}3,5\text{-}O\text{-}4)^{2-}$. *J. Am. Chem. Soc.* **2011**, *133* (14), 5244–5247.
(59) Toma, A. M.; Raţ, C. I.; Pavel, O. D.; Hardacre, C.; Rüffer, T.; Lang, H.; Mehring, M.; Silvestru, A.; Pârvulescu, V. I. Heterocyclic Bismuth(III) Compounds with Transannular N→Bi Interactions as Catalysts for the Oxidation of Thiophenol to Diphenyldisulfide. *Catal. Sci. Technol.* **2017**, *7* (22), 5343–5353.
(60) Planas, O.; Wang, F.; Leutzsch, M. H (11),. **2020**, *317* (February), 313–317.
(61) A. M. Christianson; F. P. Gabbaï, eds. T. Baumgartner, F. J. Antimony- and Bismuth-Based Materials and Applications in *Main Group Strategies Towards Functional Hybrid Materials*; Wiley, Germany, 2017, pp 405–432.
(62) Tschersich, C.; Limberg, C.; Roggan, S.; Herwig, C.; Ernsting, N.; Kovalenko, S.; Mebs, S. Gold- and Platinum-Bismuth Donor-Acceptor Interactions Supported by an Ambiphilic PBiP Pincer Ligand. *Angew. Chemie - Int. Ed.* **2012**, *51* (20), 4989–4992.
(63) Ke, I. S.; Gabbaï, F. P. σ-Donor/Acceptor-Confused Ligands: The Case of a Chlorostibine. *Inorg. Chem.* **2013**, *52* (12), 7145–7151.
(64) Tschersich, C.; Hoof, S.; Frank, N.; Herwig, C.; Limberg, C. The Effect of Substituents at Lewis Acidic Bismuth(III) Centers on Its Propensity to Bind a Noble Metal Donor. *Inorg. Chem.* **2016**, *55* (4), 1837–1842.
(65) Materne, K.; Hoof, S.; Frank, N.; Herwig, C.; Limberg, C. In Situ Formation of PBiP Ligands upon Complexation of a Mixed Phosphane/Bismuthane with Group 11 Metal Ions. *Organometallics* **2017**, *36* (24), 4891–4895.
(66) Urgin, K.; Aubé, C.; Pichon, C.; Pipelier, M.; Blot, V.; Thobie-Gautier, C.; Léonel, E.; Dubreuil, D.; Condon, S. Advanced Preparation of Functionalized Triarylbismuths and Triheteroaryl-Bismuths: New Scope and Alternatives. *Tetrahedron Lett.* **2012**, *53* (15), 1894–1896.
(67) Silvestru, C.; Breunig, H. J.; Althaus, H. Structural Chemistry of Bismuth Compounds. I. Organobismuth Derivatives. *Chem. Rev.* **1999**, *99* (11), 3277–3327.
(68) Suzuki, H; Matano, Y., eds. Chapter 2. Organobismuth(III) Compounds in *Organobismuth Chemistry*; Elsevier Science, Amsterdam, **2001**, pp 21-245.
(69) Bondi, A. Van Der Waals Volumes and Radii. *J. Phys. Chem.* **1964**, *68* (3), 441–451.
(70) Mantina, M.; Chamberlin, A. C.; Valero, R.; Cramer, C. J.; Truhlar, D. G. Consistent van Der Waals Radü for the Whole Main Group. *J. Phys. Chem. A* **2009**, *113* (19), 5806–5812.
(71) Charton, M. Organic and Biological Chemistry: The Nature of the Ortho Effect. II. Composition of the Taft Steric Parameters. *J. Am. Chem. Soc.* **1969**, *91* (3), 615–618.
(72) Artem'Ev, A. V.; Bagryanskaya, I. Y.; Doronina, E. P.; Tolstoy, P. M.; Gushchin, A. L.; Rakhmanova, M. I.; Ivanov, A. Y.; Suturina, A. O. A New Family of Clusters Containing a Silver-Centered Tetracapped $[Ag@Ag_4(\mu_3\text{-}P)_4]$ Tetrahedron, Inscribed within a N_{12} Icosahedron. *Dalt. Trans.* **2017**, *46* (37), 12425–12429.
(73) Lin, T. P.; Ke, I. S.; Gabbaï, F. P. σ-Accepting Properties of a Chlorobismuthine Ligand. *Angew. Chemie - Int. Ed.* **2012**, *51* (20), 4985–4988.
(74) Fernández, E. J.; Laguna, A.; López-De-Luzuriaga, J. M.; Monge, M.; Nema, M.; Olmos, M. E.; Pérez, J.; Silvestru, C. Experimental and Theoretical Evidence of the First Au(I)···Bi(III) Interaction. *Chem. Commun.* **2007**, *028* (6), 571–573.
(75) Tschersich, C.; Braun, B.; Herwig, C.; Limberg, C. Coordination of Noble Metals by an Ambiphilic PBiP Pincer Ligand: Metallophilic Bi-Cu and Bi-Ag Interactions. *J. Organomet. Chem.* **2015**, *784*, 62–68.
(76) Burke, P. J.; Mcmillin, D. R.; Robinson, W. R. Crystal and Molecular Structure of Bis(6,

6'-Dimethyl-2, 2'-Bipyridyl)Copper(I) Tetrafluoroborate. *Inorg. Chem.* **1980**, *19* (5), 1211–1214. Further information regarding the structure reported in this paper can be found in the SI.

(77) Parks, J. E.; Wagner, B. E.; Holm, R. H. Syntheses Employing Pyridyllithium Reagents: New Routes to 2,6-Disubstituted Pyridines and 6,6′-Disubstituted 2,2′-Bipyridyls. *J. Organomet. Chem.* **1973**, *56* (C), 53–66.

(78) Whitesides, G. M.; Casey, C. P.; Krieger, J. K. The Thermal Decomposition of Vinylic Copper(I) and Silver(I) Organometallic Compounds. *J. Am. Chem. Soc.* **1971**, *93* (6), 1379–1389.

(79) Suzuki, H; Matano, Y., eds. Chapter 5. Bismuth Compounds in Organic Transformations in *Organobismuth Chemistry*; Elsevier Science, Amsterdan, **2001**, pp 371-440.

(80) Matano, Y.; Nomura, H. Facile Oxidation of Alcohols to Carbonyl. *Angew. Chem*. **2002**, No. 16, 3028–3031.

(81) Beswick, M. A.; Lawson, Y. G.; Raithby, P. R.; Wood, J. A.; Wright, D. S. A Metallated Primary Arsine; Synthesis and Structure of $[PhAsHLi{\cdot}2tHf]_{\infty}$. *J. Chem. Soc. - Dalt. Trans.* **1999**, No. 12, 1921–1922.

(82) Janiak, C.; Chamayou, A. C.; Royhan Uddin, A. K. M.; Uddin, M.; Hagen, K. S.; Enamullah, M. Polymorphs, Enantiomorphs, Chirality and Helicity in [Rh{N,O}(η^4-Cod)] Complexes with {N,O} = Salicylaldiminato Schiff Base or Aminocarboxylato Ligands. *J. Chem. Soc. Dalt. Trans.* **2009**, *9226* (19), 3698–3709.

(83) Daniels, C. L.; Mendivelso-Perez, D. L.; Rosales, B. A.; You, D.; Sahu, S.; Jones, J. S.; Smith, E. A.; Gabbaï, F. P.; Vela, J. Heterobimetallic Single-Source Precursors: A Springboard to the Synthesis of Binary Intermetallics. *ACS Omega* **2019**, *4* (3), 5197–5203.

(84) Daniels, C. L.; Knobeloch, M.; Yox, P.; Adamson, M. A. S.; Chen, Y.; Dorn, R. W.; Wu, H.; Zhou, G.; Fan, H.; Rossini, A. J.; Vela, J. Intermetallic Nanocatalysts from Heterobimetallic Group 10-14 Pyridine-2-Thiolate Precursors. *Organometallics* **2020,** https://doi.org/10.1021/acs.organomet.9b00803.

(85) Schuster, O.; Schier, A.; Schmidbaur, H. The Quest for Complexes with a Coordinative Gold-Bismuth Bond. *Organometallics* **2003**, *22* (20), 4079–4083.

Inorganic Chemistry, 2020, 59, 10, 7103–7116. https://doi.org/10.1021/acs.inorgchem.0c00579

SYNOPSIS A series of *tris*(2-pyridyl) bismuthine ligands have been prepared whose cation and anion coordination properties can be controlled by substitution in the Py ring. They can act as intact ligands and display non-innocent reactivity, such as acting as 2-pyridyl transfer reagents, and as a result of the Lewis acidity of their Bi(III) centers, exhibiting anion dependent reactivity.